Title

Studies of Gene Expression During Memory: i) Role of Extracellular Vesicles & ii) Impact of Aging on Gene Expression in Mouse Hippocampus

Permalink

https://escholarship.org/uc/item/8rs8t1jg

Author

Tao, Yang

Publication Date

2019

Peer reviewed|Thesis/dissertation

UNIVERSITY OF CALIFORNIA

Los Angeles

Studies of Gene Expression During Memory:

i) Role of Extracellular Vesicles &

ii) Impact of Aging on Gene Expression in Mouse Hippocampus

A dissertation submitted in partial satisfaction of the requirements

for the degree Doctor of Philosophy in Molecular Biology

by

Yang Tao

2019

ABSTRACT OF THE DISSERTATION

Studies of Gene Expression During Memory:

i) Role of Extracellular Vesicles &

ii) Impact of Aging on Gene Expression in Mouse Hippocampus

by

Yang Tao

Doctor of Philosophy in Molecular Biology

University of California, Los Angeles, 2019

Professor Kelsey C. Martin, Chair

Learning and memory have long been hot topics in the field of neuroscience, not only because they play fundamental roles in human experience, but also because there are multiple diseases that are associated with deficits in learning and memory. At the cellular level, memory results from changes in the strength of the synaptic connections between neurons, and alterations in gene expression underly the persistence of many of these changes.

Translation of synaptically localized mRNAs is important for long-term synaptic plasticity. Extracellular vesicles (EVs) contain RNAs and neuronal EV secretion has been reported to be regulated by synaptic activity, which leads to the hypothesis that EVs are

transferred between cells in the nervous system and that mRNAs and microRNAs transferred through this pathway are important for local translation during neuronal plasticity. To test this hypothesis, we purified EVs from primary neuronal culture media and performed small RNA sequencing on neuronal evRNAs and their respective donor cells. We found an enrichment of small RNAs in EVs, and the composition of the small RNAs, including the miRNA profile, was distinct from that in donor cells. Our findings reveal a comprehensive map of RNAs inside neuronal EVs and identify multiple miRNAs as promising candidates for future investigation.

Normal aging often involves some level of memory impairment and as such represents a physiologically relevant manipulation of plasticity and memory, with the comparison between young and aged mice providing insights into differences in gene regulation that may be central to plasticity and memory. We performed ATAC-seq and RNA-seq on the hippocampus of young and aged mice and found that aging resulted in significant changes in the expression of genes involved in neurogenesis, immune response, and cell adhesion, and in the alternative splicing of select myelin sheath genes. We found that aged female mice had higher levels of expression of several myelin sheath genes compared to aged male mice. Chromatin accessibility analysis revealed a more open chromatin structure in the hippocampus of aged animals compared to young animals, and many of these changes occurred at repetitive elements. However, changes in chromatin accessibility were not well-correlated with changes in gene expression. Our results provide insights into the changes in gene expression that occur with aging, highlighting changes in genes important for myelin sheath maintenance, and suggest that age-related chromatin accessibility changes may play an indirect role in age-related transcriptional changes.

The dissertation of Yang Tao is approved.

Bennett G. Novitch

Douglas L. Black

Luis De La Torre-Ubieta

Thomas J. O'Dell

Kelsey C. Martin, Chair

University of California, Los Angeles

2019

DEDICATION

      This thesis is dedicated to my parents who have provided me tremendous love and emotional support throughout these years; to my partner Weiyi Wu, who made many sacrifices and compromises to help me through the hard times; to my mentor Kelsey Martin, who gave me valuable guidance not only on research but also on my career and life; to Martin lab members and collaborators, without whom I would not be able to carry my research this far; and to my committee members, for their help and advice on my graduate work.

TABLE OF CONTENTS

LIST OF FIGURES

LIST OF TABLES

ACKNOWLEDGEMENTS

VITA

EDUCATION

- **Biological Chemistry, University of California, Los Angles**   **9/2013-Now**
  Ph.D. candidate, Mentor: Dr. Kelsey Martin
- **School of Life Sciences, Peking University**   **9/2009-7/2013**
  Bachelor of Science in Biology, awarded in July 2013
- **Cross-disciplinary Scholars in Science & Technology Summer Program, UCLA**   **7/2012-9/2012**
  Mentor: Dr. X. William Yang, Center for Neurobehavioral Genetics, UCLA

RESEARCH EXPERIENCE

- **Graduate Student**   **7/2014-Now**
  PI: Dr. Kelsey Martin, Biological Chemistry, University of California, Los Angeles
  Project1: Understanding RNA transfer via extracellular vesicles during neuronal synaptic plasticity
  Conducted a novel study to identify the function of extracellular vesicles in intercellular RNA transfer and neuronal synaptic plasticity
  Project2: Understanding how does aging alter the landscape of chromatin accessibility and pattern of gene expression in the hippocampus
  Performed ATAC-seq and RNA-seq on the hippocampus of young and aged mice of both sexes
- **Research Assistant**   **9/2012-7/2013**
  PI: Dr. Yan Zhang, School of Life Sciences, Peking University
  Project: Investigating the role of SHANK3 in Alzheimer's disease
  The relationship between Shank3 and micro-RNA 3425P was being investigated with molecular and cellular approaches. The role of Shank3 was being detected in cultured neurons from Alzheimer mice.
- **Summer Student**   **7/2012-9/2012**
  PI: Dr. X. William Yang, Department of Psychiatry & Biobehavioral Sciences, UCLA
  Project: Identifying interacting proteins of the N-terminal domain of Huntingtin
  The N-terminal 17 amino-acid peptide was cloned and expressed as bait for a yeast-two hybrid screen. A protein involved in cilia biology was identified as a potential interactor of Huntingtin.
- **Research Assistant**   **10/2010-7/2012**
  PI: Dr. Yi Rao, Laboratory of Social Behavior and Cognition, Peking University
  Project: Genetic and neuronal bases of Mirror Neuron
  This project was supported by National University Student Innovation Incentive Program. Two paradigms were designed and used to test the ability of Theory of Mind and imitation respectively in 1000 twin pairs.

OTHER EXPERIENCE

- **President, UCLA Advanced Degree Consulting Club**   **9/2017-9/2018**
  Led the executive board, launched workshop serious and weekly interview preparation events, explored fund raising strategies
- **Technology Fellow, UCLA Technology Development Group**   **6/2016-9/2017**
  Performed technologies evaluation, market analysis, patent and regulation research, interviewed industry professionals and stakeholders, composed evaluation forms, prepared pitch decks
- **Teaching Assistant, Life Science 3, UCLA**   **1-4/2015, 3-6/2016**
  Organized discussion sections, held office hours, corrected assignments and exams
- **Teaching Assistant, Genetics**   **2/2013-7/2013**
  Organized discussion classes, helped students with presentation, corrected assignments
- **Selected Speaker, CSST Summer Program, UCLA**   **9/2012**
  Presented the results of summer project to the CSST group on CSST Closing Ceremony

SKILLS AND ACTIVITIES

- **Language:** Fluent in Mandarin and English
- **Computer:** Skilled in MS Office, C programing, MATLAB
- **Interests:** Ping-Pong, snowboarding, trampoline, music

x

AWARDS AND HONORS

- **Dissertation Year Fellowship, UCLA** — **2018-2019**
- **WhitCome Pre-doctoral Fellowship, UCLA** — **2015-2017**
- **CSC-UCLA Scholarship, China Scholarship Council** — **2013**
- **First Prize, Summer Scholarship, PKU** — **2013**
- **Best Student Presenter, CSST Summer Program, UCLA** — **2013**
- **Best Presenter, Supervised Independent Study, PKU** — **2012**
- **SINO Scholarship, Education Abroad Program, PKU** — **2012**
- **Fellowship, National College Student Innovation Incentive Program** — **2011**

CHAPTER 1 – INTRODUCTION

Learning and memory

Learning describes the process of acquiring external information. Memory describes the

storage of that information. Learning and memory have long been hot topics in the field of

neuroscience, not only because they are so fundamental to the human experience, but also

because there are multiple diseases that are associated with deficits in learning and memory.

For instance, lesion of the medial temporal lobe affects recent memories and lesion of the

hippocampus is associated with temporally-graded retrograded amnesia (Frankland and

Bontempi, 2005). Neurodegenerative diseases, such as Alzheimer's disease, are often

associated with learning and memory impairment, eventually leading to dementia (Fischer et

al., 2007). In addition to disease states, learning disabilities and memory deficits can also occur

in healthy human beings under certain circumstances, including stress, sleep deprivation, and

normal aging.

Compared with many other mental processes, learning and memory are relatively easy

to assess in humans and in non-human animal models. Multiple animal models have been used

to study the mechanisms of learning and memory, with mice being particularly common

because they are amenable to genetic manipulation and to *in vivo* imaging and

electrophysiology. Learning and memory are supported by multiple separate brain regions,

including the hippocampus, amygdala, cerebellum and cortex. For instance, fear memory

involves the hippocampus, amygdala and prefrontal cortex. Procedural memory involves the

cerebellum. Among these structures, the hippocampus is one of the best-studied systems

because its anatomical structure, with distinct cell body layers and projection pathways, is ideal for electrophysiological investigation (Ho et al., 2011).

Synaptic plasticity

At the cellular level, memory results from changes in the strength of the synaptic connections between neurons. There are two types of synaptic plasticity, short-term plasticity, which lasts from milliseconds to minutes and does not require protein synthesis, and long-term plasticity, which lasts from minutes to hours and days, and requires new protein synthesis (Goelet et al., 1986). Synaptic plasticity involves changes in the pre- and post- synaptic compartments, as well as at the synaptic cleft (e.g. through changes in adhesion molecules).

In the pre-synaptic compartment, the probability and rate of neurotransmitter-containing synaptic vesicle release can be regulated in an activity-dependent manner. In the post-synaptic compartment, the localization of NMDA receptors and AMPA receptors on the plasma membrane is regulated by activity. Extracellular matrix (ECM) between the pre- and post- synapses is composed of collagens, proteoglycans and glycoproteins. The molecules that keep the pre- and post- synapses together are cell adhesion molecules (CAMs). ECM and CAMs are not only important for keeping the integrity of synapses but are also important for synaptic plasticity formation (Benson et al., 2000; Dityatev and Schachner, 2003). For instance, cadherins are enriched at synapses. They not only function as adhesion molecules but are critical for synaptic plasticity through recruitment and stabilization of AMPA receptors at synapses (Nuriya and Huganir, 2006; Tai et al., 2008).

For long-term plasticity, new RNA synthesis is required, which involves synapse to nucleus signaling (Herbst and Martin, 2017). This retrograde signaling here includes fast calcium influx and electrochemical signaling as well as the slow transport of proteins through the dendrite to the soma and into the nucleus. The newly transcribed RNAs can then be transported from the nucleus to distal dendrites and synapses. mRNAs undergo activity-dependent local translation, and microRNAs have been shown to regulate the local transcriptome (Hu and Li, 2017). In summary, activity-dependent, bidirectional communication between synapses and nucleus is able to modify the local proteome at distal synapses, enabling long-lasting strengthening or weakening of specific synapses within a given neuron.

Extracellular vesicles

Many cell types have been shown to release extracellular vesicles (EVs) of endosomal origin (exosomes) and plasma membrane origin (microvesicles, MVs) into the extracellular environment (Johnstone, 2006). EVs were first identified in cultured reticulocytes in 1983 (Harding and Stahl, 1983; Pan and Johnstone, 1983). Subsequently, EVs have been successfully purified from the culture media of various cell types and body fluids (Raposo and Stoorvogel, 2013a). These vesicles were called exosomes and their secretion was thought to be a result of fusion of multivesicular bodies (MVBs) with the plasma membrane. MVBs are late endosomes containing intraluminal vesicles (ILVs) formed by inward budding of the limiting membrane of endosomes. When MVBs fuse with the plasma membrane, the ILVs are released into the environment and are referred to as exosomes. However it was later found that in addition to exosomes, cells also release vesicles that are directly shed from the plasma membrane, which

are called MVs or budding vesicles (Booth et al., 2006). Exosomes are generally smaller in size (30-150 nm) while MVs can vary from 100-1000nm. However, currently there is no effective way to separate these two populations of vesicles. Exosomes and MVs together are called extracellular vesicles (EVs). After being released, EVs can bind to recipient cells and undergo endocytosis or direct fusion with the plasma membrane to deliver the contents of the EVs to the recipient cells.

Proteomic studies found that EVs contain proteins involved in MVB biogenesis (van Niel et al., 2006), tetraspanins (Zöller, 2009), as well as proteins that are associated with lipid rafts (Wubbolts et al., 2003). Moreover, recent studies have reported that mRNAs and microRNAs are also actively sorted into EVs and can alter gene expression in recipient cells (Pegtel et al., 2010; Valadi et al., 2007; Villarroya-Beltri et al., 2013). EVs were thought to mainly function as a way to discard obsolete molecules (Harding et al., 2013), however the discovery of protein and RNA transfer between cells through EVs implies their potential role in intracellular communication. Tumor cells release EVs that can promote tumor progression by inducing the expression of angiogenic associated genes (Hood et al., 2011), which also makes EVs promising candidates for circulating cancer biomarkers (Lane et al., 2018). Antigen-presenting cells such as dendritic cells and B cells secrete EVs that carry the MHC-II dimers bound to antigen peptide. These EVs can activate T cells and suppress tumor growth (Muntasell et al., 2007; Zitvogel et al., 1998).

While EVs have been most extensively studied in the immune system, recent studies have described EVs in the nervous system (Korkut et al., 2013; Rajendran et al., 2014). Several critical findings were in fly system. Synaptotagmin 4 (Syt4) and Evenness Interrupted (Evi) were

shown to be transmitted from presynaptic cell to postsynaptic cell through EVs at the

Drosophila neuromuscular junction, contributing to activity-dependent synaptic growth (Koles

et al., 2012; Korkut et al., 2013). Drosophila Arc1 proteins can form virus-like capsids containing

darc1 mRNA and be transferred through EVs at the neuromuscular junction, which was shown

to be required for synaptic plasticity (Ashley et al., 2018). In mammalian systems, cultured

cortical neurons secrete EVs that contain proteins important to synaptic function, including

GluR2/3 (Fauré et al., 2006), as well as proteins that are associated with neurodegenerative

diseases, PrPc and α-synuclein (Schneider and Simons, 2013). Furthermore, neuronal EV release

has been shown to be regulated by calcium influx and glutamatergic synaptic activity (Lachenal

et al., 2011). Transfer of Arc proteins and mRNAs via EVs have been detected in cultured

hippocampal neurons, with the transferred Arc mRNAs being translated in an activity-

dependent manner (Pastuzyn et al., 2018). These results suggest that EVs may play a role in

synaptic plasticity and that they may regulate neuronal plasticity and memory formation

through the inter-cellular transfer of synaptic proteins and RNAs. Translation of synaptically

localized mRNAs is important for long-term synaptic plasticity. The traditional view is that

transcripts are transported from the nucleus to the synapses where they undergo local

translation. The finding that EVs contain RNAs and that neuronal EV secretion is regulated by

synaptic activity leads to the hypothesis that EVs are transferred between cells in the nervous

system in an activity dependent manner and that mRNAs and microRNAs transferred through

this pathway are important for local translation during neuronal plasticity.

Aging

Aging is a naturally occurring process that is often accompanied by impairments in learning and memory. However, the cause of these impairments is not clear yet. Understanding how the brain changes during aging can help us to better understand the molecular and cellular basis of learning and memory.

It is known that many changes occur during brain aging. These changes include, but are not limited to, cognitive decline, brain atrophy, blood brain barrier breakdown, activation of the immune system, decreased neurogenesis, altered synaptic connectivity and gene expression changes.

The cognitive decline that occurs during aging affects daily life. Such changes include declined conceptual reasoning, impaired memory, slowed processing speed and reduced selective attention. In contrast, other cognitive abilities don't change during aging, such as vocabulary and general knowledge (Harada et al., 2013). Some of these deficits, e.g. impaired memory, have also been validated in animal models. It is important to know that great heterogeneity exists among elderly in terms of the speed of their decline. For instance, in a human study, a sample of 1049 participants with a mean age of 75 years, were followed for a median length of 8 years (Hayden et al., 2011). The participants were tested annually for their cognitive function using neuropsychological tests, including, but not limited to, episodic memory, working memory and visuospatial ability. The statistical analysis separated the participants into slow and fast decline classes, with the fast decliner declining about four times faster than the slow decliner. Similar phenomena have been observed in mice tested on the Morris water maze (Pawlowski et al., 2009).

Historically, before advanced tissue processing techniques and stereological principles were developed, it was believed that profound neuronal loss occurred in hippocampus and prefrontal cortex during human brain aging, and that this was the cause of learning and memory deficits (Ball, 1977; Brody, 1955). However, in the 1980s, more advanced technologies revealed that there is no significant cell loss during normal aging in humans, non-human primates and rodents (Burke and Barnes, 2006). Despite the relatively stable maintenance of the number of neurons, MRI studies demonstrated that in humans the gross brain volume decreases 0.2-0.5% annually, with the hippocampus showing an annual atrophy rate of 0.79%-2.0% (Fjell et al., 2009). This shrinkage could be due to decreases in neuronal size, loss of neuronal projections etc. In terms of the change of numbers of synapses during aging, the answer is much more complicated. It is highly dependent on which approach is used (immunoblotting, proteomics, electron microscopy etc.) and which brain region is studied (Petralia et al., 2014). For CA3-CA1 synapses, the total number of synapses does not change with aging but aged learning-impaired rats showed a 30% reduction of post synaptic density (PSD) size (Nicholson et al., 2004). This loss in PSD size could potential cause synaptic dysfunction.

For many years, it was believed that the central nervous system (CNS) was isolated from the immune system by the blood-brain barrier (BBB) and that the CNS was immunologically inert. However, recent data suggests that CNS is immune-competent and actively interacts with the peripheral immune system (Carson et al., 2006). Interestingly, immune activation is one of the most prominent feature of brain aging (Lucin and Wyss-Coray, 2009). It has been reported in multiple species, including in human post-mortem tissues and in rodents, that sensitized

microglia are a primary source of the neuroinflammatory responses during aging, with up-regulation of immune activation makers including major histocompatibility complex II (MHC II) and complement receptor 3 (CD11b, Barrientos et al., 2015). There is still debate in the field regarding the cause of neuroinflammation during aging. Possibilities include changes in hormone levels, breakdown of the blood brain barrier, and altered neuronal inhibitory control over microglia. How this immune activation is related to cognitive deficits remains unclear.

Another known cellular change during brain aging is the depletion of neural stem cells. In the mouse dentate gyrus, between 3 weeks and 2 years of age, there is a 100-fold decrease in the number of quiescent neural progenitors and a 15-fold decrease in the number of amplifying neural progenitors (Encinas et al., 2011). This decrease in the number of neural progenitors occurs shortly after birth and continues through the life span. One hypothesis is that the loss of neural stem cells in the hippocampus might lead to a decline in the production of new neurons, contributing to age-related cognitive deficits. However, over the last two decades, there has been significant controversy in the neuroscience field as to whether and to what extend adult neurogenesis occurs in human (Andreae, 2018). Thus, the significance of the decreased number of neuronal progenitors during aging remains unclear.

At the molecular level, several studies have investigated changes in gene expression during brain aging. In the context of basal level gene expression changes, the neuroinflammatory pathway has been shown to be altered in mouse and human hippocampus during aging (Soreq et al., 2017; Stilling et al., 2014). However, most of these expression profiling studies were either based on microarray analysis or on RNA-sequencing with low sequencing depth. Thus, many smaller amplitude gene expression changes would not be

detected. Less is known about activity-dependent gene expression changes during aging, although one study has shown that the immediate early gene Arc failed to be transcriptionally induced after spatial memory tests in aged rats (Penner et al., 2011).

Sex Differences

In the history of animal studies, there is a great bias towards using male animals and ignoring female animals, especially in the neuroscience studies. It is reported that there are 4.5 times more single-sex studies of male animals than there are of female animals (Beery and Zucker, 2011). Only 22% of the neuroscience animal studies include both sexes, however very few of these studies analyze results by sex. The main consideration that has led to the preponderance of studies on male as opposed to female animals is that fluctuating hormone levels can leads to heterogeneity in female animals. However, in many cases, the findings in male cannot be generalized to female. For brain aging specifically, many differences exist between males and females. Several behavioral tests have detected gender-specific, age-dependent cognitive changes in humans (León et al., 2016; McCarrey et al., 2016; Wang et al., 2018). In terms of which gender performs better during aging, the results are dependent on which protocols are being used, which age groups are being studied and how the age adjustment is being done. For instance, it was reported that aged men outperform women on measures of spatial ability while aged women outperform men on measures of reasoning and verbal ability (McCarrey et al., 2016). PET studies of normal male and female humans showed that in terms of brain metabolism, female brain ages slower than male brain (Goyal et al., 2019). MRI studies showed that there is more brain atrophy with aging in male compared to

female (Pruessner et al., 2001; Xu et al., 2000). To our knowledge, no one has carefully

characterized age-dependent gene expression changes in hippocampus in female animals.

ATAC-Seq

ATAC-Seq stands for Assay for Transposases Accessible Chromatin Sequencing

(Buenrostro et al., 2015). This technique uses hyperactive transposase Tn5 to probe for

chromatin accessibility. Tn5 can fragment and tag the open chromatin region with sequencing

adapters at the same time. The resulting DNA fragments are then amplified and sequenced.

Compared to other technologies used to assess chromatin accessibility such as DNase-Seq and

FAIRE-Seq, ATAC-Seq is much faster, simple and requires much less starting material

(Buenrostro et al., 2015).

The opening of the chromatin at promoter and enhancer regions is required for active

gene transcription (Li et al., 2007). Studies using ATAC-seq to profile chromatin accessibility

changes during neuronal activity (Su et al., 2017) and neurogenesis (De La Torre-Ubieta et al.,

2018) showed that changes in chromatin accessibility are correlated with transcriptional

changes. Chromatin structure is regulated by multiple factors, including nucleosome

positioning, epigenetic modifications, and binding of transcriptional factors, chromatin

remodelers and non-coding RNAs (Han and Chang, 2015; Klemm et al., 2019). By mapping

chromatin accessibility with ATAC-Seq, we can infer the contribution of these factors to

differential gene expression under different conditions and stimulations.

CHAPTER 2 – Profiling of RNAs in Neuronal Extracellular Vesicles

Abstract

Extracellular vesicles (EVs) have been successfully purified from the culture media of various cell types and body fluids and their function has been extensively studied in several systems, including the immune system and the nervous system. However, most of these studies have focused on one or a few target proteins or RNAs present in EVs. In this study, we set out to use RNA sequencing approaches to identify the population of small RNAs present in neuronal EVs. Towards this end, we purified EVs from primary neuronal culture media and performed small RNA sequencing on neuronal evRNAs and their respective donor cells. We found an enrichment of small RNAs in EVs, and the composition of the small RNAs, including the miRNA profile, was distinct from that in donor cells. Our findings reveal a comprehensive map of RNAs inside neuronal EVs and identify multiple miRNAs as promising candidates for future investigation.

Introduction

Virtually all cell types have been shown to release extracellular vesicles (EVs) of endosomal origin (exosomes) and plasma membrane origin (microvesicles) into their extracellular environment *in vitro* and *in vivo* (Raposo and Stoorvogel, 2013b). Moreover, several studies have demonstrated that cytosolic proteins undergo regulated sorting into EVs secreted by donor cells and these EVs are subsequently taken up by recipient cells (Théry et al., 2002), suggesting a functional role for EVs in intercellular communication. In addition, recent

11

studies have reported that mRNAs and microRNAs (miRNAs) are also actively sorted into EVs (Villarroya-Beltri et al., 2013) and can alter gene expression in recipient cells (Valadi et al., 2007; Pegtel et al., 2010). These findings suggest that EV-mediated transfer of RNAs provides a novel mechanism of gene regulation, one in which neighboring cells can alter the local transcriptome and proteome of one another.

While EVs have been most extensively studied in the immune system, recent studies have described EVs in the nervous system (Korkut et al., 2013; Rajendran et al., 2014). Cultured cortical neurons secrete EVs that contain proteins important to synaptic function, including GluR2/3 (Fauré et al., 2006), as well as proteins that are associated with neurodegenerative diseases, PrPc and α-synuclein (Schneider and Simons, 2013). Furthermore, neuronal EV release has been reported to be regulated by calcium influx and glutamatergic activity (Lachenal et al., 2011). These results suggest that EVs may play a role in synaptic plasticity and that they may regulate neuronal plasticity and memory formation through the transfer of synaptic proteins and RNAs. Recently, it was reported that in *Drosophila*, several proteins, including SYT4, EVI and ARC1, were transferred from motor neurons to muscle via EVs at the neuromuscular junction, which was critical for activity-dependent synaptic growth (Ashley et al., 2018; Koles et al., 2012; Korkut et al., 2013).

To date, the RNAs in neuronal EVs have not been well characterized. Translation of synaptically localized mRNAs is important for long-term synaptic plasticity. The traditional view is that transcripts are transported from the nucleus to the synapses where they undergo local translation. The finding that EVs contain RNAs and that neuronal EV secretion is regulated by synaptic activity leads to the hypothesis that EVs are transferred between cells in the nervous

system and that mRNAs and microRNAs transferred through this pathway may contribute to local translation during neuronal plasticity (Fig. 1-1A).

In this study, we purified EVs from rat primary neuronal culture media by differential ultracentrifugation and demonstrated that these EVs were taken up by recipient neurons by endocytosis. Small RNA sequencing was performed on RNAs purified from neuronal EVs as well as their donor cells and we found the RNAs inside neuronal EVs were very different from those in donor cells or from EVs generated from other cell types. Interestingly, several miRNAs that we found to be enriched in neuronal EVs have been reported to play critical roles in neuronal development and neurite growth.

Materials and Methods

Cell culture

Mouse neuroblastoma N2a cells were cultured in DMEM supplemented with 10% FBS in 175cm^2 cell culture flasks. Cells were passaged every 2 days.

For primary neuronal cultures, Corning 100mm cell culture dishes were coated with poly-D-lysine (0.1mg/mL in 0.1M Borate buffer, pH 8.5) overnight in the incubator (37 ℃, 5% CO$_2$). The next day, dishes were washed 3 times with warm PBS and allowed to dry. Forebrains from P0 rat pups were dissected on ice, chopped into small pieces and incubated in trypsin buffer (10mL HBSS, 0.25% trypsin, 1mg DNase, 1mM CaCl$_2$) at 37 ℃ for 15min. The trypsin buffer was then removed and forebrain pieces were washed with trypsin inhibition buffer (10mL HBSS, 10mg trypsin inhibitor) twice, each time with 5mL for 5min at room temperature. Then 10mL plating medium was added (200mL Neurobasal A medium, 4mL EV depleted B27,

0.5mL Glutamax, 0.2mL 25mM glutamate, 0.2mL 25mM beta-mercaptoethanol) and the tissue was triturated 10 times with a P1000 pipette to dissociate the cells. Cells of one forebrain, including both neurons and glial cells, were plated onto one coated 100mm dish. On average $9*10^6$ cells were plated per 100mm dish. The next day, to remove dead cells and cell debris, the plating medium was removed and 10mL fresh plating medium was added. At DIV7, 5mL feeding medium (200mL Neurobasal-A medium, 4mL EV depleted B27) was added. The B27 for the plating media and feeding media was ultracentrifuged at 120,000g overnight at 4 ℃ to remove EVs. Use of animals in this study followed the recommendation of and protocol approved by the UCLA Institutional Animal Care and Use Committee.

Extracellular Vesicle Purification

For N2a cells, cells were washed with warm PBS and fresh DMEM medium (no FBS) was added 12 hours before medium collection. For primary neuronal cultures, medium was collected at DIV 16.

Culture medium was centrifuged at 2000*g for 10min at 4 ℃ and then centrifuged at 20,000g for 20min at 4 ℃. The supernatant was then passed through a 0.22μm filter and centrifuged at 100,000g for 70min at 4 ℃. The pellet was then resuspended in PBS. To deplete extra-vesicular proteins and RNAs, EVs were first treated with 0.25% trypsin for 15min at 37 ℃. After trypsin was deactivated with 5μg/μL trypsin inhibitor, EVs were then treated with $2.5*10^5$ gel units/mL micrococcal nuclease (MNase) for 15min at 37 ℃. Purified EVs were stored at 4 ℃ for short term and -20 ℃ for long term.

Western Blot

If the EV protein of interest is a transmembrane protein, then the EVs were not treated with trypsin. EVs were mixed with RIPA buffer (containing protease and phosphatase inhibitors). For donor cells, after medium was harvested, cells were washed with cold PBS and scraped and lysed in RIPA buffer (containing protease and phosphatase inhibitors). Protein concentration was determined using Thermo Fisher Pierce BCA Protein Assay Kit. 4X sample loading buffer (0.2M Tris-HCl pH 6.5, 4.3m glycerol, 8.0% (w/v) SDS, 6mM bromophenol blue, 0.4M DTT) was added and samples were boiled at 95-100 ℃ for 10min. The samples were then aliquoted and stored at -20 ℃. 10μg of EV proteins or 30μg of cellular proteins was loaded onto each lane. After transfer, blots were incubated in LI-COR Odyssey TBS blocking buffer for 1 hr at room temperature. Then blots were incubated in primary antibody at 4 ℃ overnight, washed in TBST and incubated in secondary antibody for 2 hr at room temperature. Antibodies being used are: anti-Alix (Cell Signaling, 2171S), anti-FLOT1 (BD Biosciences, 610820), anti-GluR2 (EMD Millipore, MAB397), anti-CNX (Abcam, ab10286), anti-GM130 (BD Biosciences, 610822), anti-HA (EMD Millipore, 11867423001), anti-GFP (Rockland, 600-401-215).

EV transfer

For direct EV labeling, PKH26 (Sigma, MINI26-1KT) was used according to the manufacturer's protocol. In controls, the same volume of vehicle (PBS) was labeled. After labeling, EVs or PBS control were ultracentrifuged at 100,000g for 70min at 4 ℃ and the pink pellet was resuspended in PBS. This step was repeated 3 times. After 3 washes, a pink pellet was still visible for EVs but not for the PBS control. For CD63-HA-GFP expression, N2a cells were

transfected with CD63-HA-GFP construct and EVs were purified from culture medium two days after transfection.

For uptake tests, EVs needed to be well resuspended and disassociated. As necessary, mild sonication was used to dissociate the pellet. For EVs pelleted from 40mL culture medium, 200μL PBS was used for resuspension and 20μL of the resuspended EVs were used for one well of a 24 well cell culture plate. Recipient cells were incubated with labeled EVs or with PBS control. To inhibit endocytosis, recipient cells were incubated with 50uM dynasore (EMD Millipore, D7693) in 0.05% DMSO for 20 min before incubation with EVs.

For confocal microscopy imaging, 2 hours after incubation, recipient cells were washed with PBS 3 times, then fixed with 4% paraformaldehyde for 10min, permeabilized with 0.1% Triton X-100 for 10min and blocked with 1% BSA for 1 hr. Cells were incubated with primary antibodies overnight at 4 °C, followed by an incubation with secondary antibodies for 2 hr. Zeiss LSM700 confocal microscope was used to acquire images.

For live imaging, Zeiss spinning disk confocal microscope was used. For 5-20 minute time lapse movies, images were taken every 3 minutes. For 20-70 minute time lapse movies, images were taken at every 5 minutes. For 70-150 minute time lapse movies, images were taken every 10 minutes.

EV RNA Purification

EVs were treated with trypsin and MNase to remove extravesicular RNAs. Total RNAs were then purified from EVs and donor cells using mirVana miRNA Isolation Kit (Thermo Fisher Scientific). RNA concentration was determined using Qubit (Thermo Fisher Scientific). We

typically purified 250-300ng EV RNAs from 50mL culture medium. Bioanalyzer analysis was

performed in the UCLA Center for Systems Biomedicine.

TaqMan MicroRNA Assay was performed for miRNA 124a (Thermo Fisher Scientific,

Assay ID 001182) and snoRNA 202 (Thermo Fisher Scientific, Assay ID 001232).

Small RNA sequencing

After RNAs were purified, small RNA libraries were prepared using the TruSeq Small RNA

Library Preparation kit (Illumina). Size selection was then performed using AMPure beads

(Beckman Coulter) to remove smaller DNA fragments at a ratio of samples:beads= 1:1.8.

ScreenTape (Agilent) analysis was performed before and after to confirm that the size selection

worked. Paired-end 50bp sequencing was performed using the Illumina HiSeq2500 at the UCLA

Broad Stem Cell Research Center Sequencing Core.

Sequencing data analysis

We applied an iterative alignment strategy (Yuan et al., 2016). In short, unmapped

sequences from the previous alignment were used for the mapping of the next RNA database.

The sequences were first mapped to miRbase (http://www.mirbase.org), then piwiRNABank

(http://piwiRNAbank.ibab.ac.in), and finally the entire rat genome (Rnor_5.0). Expression

profiles were normalized to reads per million mapped reads (RPM) for comparing purpose. For

downstream analysis, we only focused on reads that were less than 50nt. For analyzing

differential expression of miRNAs in EVs and donor cells, we used DESeq2.

Results

EV are purified from culture medium using ultracentrifugation

Several EV purification techniques have been reported, including, but not limited to, ultracentrifugation, immunoaffinity capture, precipitation using water-excluding polymers, and size-based isolation (ultrafiltration, sequential filtration, exclusion chromatography et al., Li et al., 2017). When choosing the technique most appropriate for our study, yield was the greatest concern. Immunoaffinity capture is very specific, but the yield is low and only a subset of EVs is captured depending on the antigen being used for immunoaffinity purification. Moreover, since the protein composition of neuronal EVs is largely unknown, immunoaffinity capture is not feasible. Several commercial kits are available for EV precipitation, but the purity and yield of EVs are questionable. Size-based isolation of EVs also has relatively low yield. Thus, we decided on ultracentrifugation, which is relatively labor intensive but allows good yield.

We wanted to use primary neuronal cultures that were sufficiently mature and displayed synaptic activity, which occurs typically between 14-21 days in culture. However, based on our tests, we found that mouse primary cortical cultures in 100mm dishes did not reliably remain healthy for over 14 days. Thus, to culture primary neurons at large scale, we used rat cortical cultures instead of mouse. At DIV16, the medium of rat primary neuronal cultures was harvested, centrifuged at low speed and filtered to remove dead cells and cell debris, and was then ultracentrifuged to pellet EVs (Fig. 1-1B). The visible pellet was resuspended and processed as needed. Considering that proteins and RNAs outside of EVs may contaminate the preparation, trypsin and micrococcal nuclease were used to digest these contaminants (Fig. 1-1C). However, trypsin would also digest the extracellular portion of the

18

transmembrane proteins and might affect downstream analysis, therefore trypsin was only

applied when the integrity of EV transmembrane proteins was not required.

To analyze the purity of our EV preparation, we performed immunoblotting. Although

no markers are exclusively present in EVs, a number of proteins have been shown to be

enriched in EVs, including Alix, Flotillin-1 and CD63 (Raposo and Stoorvogel, 2013b). The EVs

purified from rat primary neuronal culture medium were immunopositive for the EV marker

proteins Alix and Flottillin-1 but were immunonegative for the ER marker calnexin and the Golgi

marker GM130 (Fig. 1-2A). Glutamate Receptor 2 (GluR2) has been reported to be present in

neuronal EVs (Fauré et al., 2006) and its presence was verified in our EV preparation as well

(Fig. 1-2A). To prove that EVs were intact and that the EV proteins were indeed inside EVs, we

performed a trypsin digestion test (Fig. 1-2B). EVs were treated with trypsin, then followed

either by the addition of detergent to permeabilize the EV membrane, subjecting proteins

inside EVs to trypsin digestion, or trypsin was deactivated first before EV lysis. Our results

showed that Alix was digested in the presence of active trypsin and detergent but was

protected from trypsin digestion when the EV membrane was intact, indicating that Alix was

located inside the EVs (Fig. 1-2C). Analysis of neuronal EVs by electron microscopy showed that

the majority of purified vesicles were between 30-150nm in diameter and had a cup-shaped

morphology that was similar to that described in previous studies (Fig. 1-2D). Together, these

data indicate that we were able to successfully purified EVs from primary neuronal culture

medium by ultracentrifugation.

EVs are taken up by N2a cells and cultured neurons through endocytosis

Before analyzing neuronal EV cargos, we set out to demonstrate that EVs were indeed transferred between cells. We first tested whether EVs were delivered from donor cells to recipient cells in Neuro2a (N2a) cells. N2a cells are a mouse neuroblastoma cell line that is fast growing and that can be cultured in large scale, greatly facilitating EV purification and thereby presenting a tractable system for initial testing. We purified EVs from N2a cell culture medium and labeled EVs with PKH26 dye (Morelli et al., 2004). Labeled EVs were washed extensively to ensure that all free PKH26 dye was removed. Recipient N2a cells were then incubated with labeled EVs for 2 hours. Subsequent imaging showed that recipient N2a cells displayed punctuate staining, suggesting that EVs were taken up into recipient N2a cells through endocytosis (Fig. 1-3A). Direct fusion of EVs with the plasma membrane of recipient cells might also occur, but then we would expect the signal to be diffused and dim, making it difficult to observe. Direct labeling of N2a cells with PKH26 showed an even staining of the cell plasma membrane, indicating that the punctate signal we observed represented internalized EVs rather than from direct labeling of cells with unincorporated PKH26 dye.

To further test if EV cargos were secreted with EVs and taken up by recipient cells, we expressed CD63-HA-GFP in N2a cells. EVs isolated from the transfected N2a cells were immunopositive for HA and GFP (Fig. 1-3B), indicating that CD63-HA-GFP proteins were sorted into EVs. Confocal imaging of the transfected cells showed CD63-associated intracellular vesicular structures, which might represent multivesicular bodies or lysosomes (Fig. 1-3C). After 2 hours of incubation with labeled EVs, recipient N2a cells exhibited punctate GFP signal (Fig. 1-3C). To further test whether the EVs were indeed being taken up through endocytosis, we pre-treated the recipient cells with the endocytosis inhibitor dynasore, which blocked the uptake

(Fig. 1-3C). The interaction of EV membrane proteins with recipient cell membrane proteins has been reported to be critical for EV uptake (Mulcahy et al., 2014). To test this, we pre-treated the EVs with trypsin, which also blocked uptake (Fig. 1-3C). The GFP portion of the CD63-HA-GFP protein was intracellular, thus it would not be digested by trypsin. Therefore, the disappearance of GFP signal in recipient cells when EVs were trypsinized indicated that EV membrane proteins were required for their uptake into recipient cells. We further performed a time course of EV uptake using live imaging of N2a cells incubated with CD63-HA-GFP containing EVs (Fig. 1-3D). The fluorescent intensity inside recipient cells increased as incubation time increased, indicating that EV uptake was time dependent.

To demonstrate EV transfer in primary neuronal cultures, we applied the PKH26 labeling system, because neurons are not as easily transfected as N2a cells. EVs isolated from DIV 16 rat primary cortical neuronal culture medium were labeled with PKH26 and the recipient DIV 16 cultures were incubated with labeled neuronal EVs for 2 hours. Confocal microscopy imaging showed that the labeled EVs were taken up by recipient neurons (immunopositive for Map2) as well as glial cells (Fig 1-4). Pre-treatment of the recipient cells with the endocytosis inhibitor dynasore blocked the uptake, indicating EVs were taken up through endocytosis.

In summary, these data showed that N2a cells as well as cultured primary rat neurons secreted EVs into the extracellular environment and that these EVs could be taken up by recipient cells through endocytosis and this uptake was mediated by protein-protein interactions.

Specific small RNAs are enriched in neuronal EVs

21

To identify the RNA cargos inside neuronal EVs, we purified total RNAs from neuronal EVs as well as from donor cells (Fig. 1-5A). It has previously been reported that RNA quality and yield differed substantially depending on RNA isolation methods (Eldh et al., 2012). We have compared the RNeasy Mini Kit (Qiagen) and the MirVana miRNA Isolation Kit (Thermo Fisher Scientific) for EV RNA purification, and the RNA yield from the MirVana kit was much higher. To test the quality and purity of purified RNAs, we quantified miRNA 124a and small nucleolar RNA 202 in EVs and donor cells using TaqMan Small RNA Assay (Thermo Fisher Scientific). miRNA 124a has been shown to be sorted into neuronal EVs (Morel et al., 2013) and was present in our EV RNAs as well. SnoRNA 202, on the other hand, being a nucleolar RNA and not expected to be sorted into EVs, was detected only in donor cells but not in EVs. In addition, bioanalyzer analysis of the total RNAs showed a lack of 18S and 28S ribosomal RNAs in EVs (Fig. 1-5B). Bioanalyzer analysis also revealed that EV RNAs were mainly comprised of small RNAs, which led us to further analyze the small RNA population in EVs and donor cells (Fig 1-5B). Bioanalyzer considered RNAs with a size between 10nt to 40nt miRNAs, which were 29% of small RNAs in donor cells and 58% of small RNAs in EVs as quantified by Bioanalyzer. The percentage of miRNAs in donor cells was lower because of the existence of tRNAs (around 70nt - 90nt) and other small rRNAs. tRNAs and other small rRNAs were also present in neuronal EVs but the percentage was much smaller compared to the donor cells. The different RNA composition in EVs and donor cells suggests that there is selective sorting of RNAs into EVs.

EV miRNA profile is distinct from cellular miRNA profile

We further profiled small RNAs in EVs and donor cells using deep sequencing. The RNA libraries were size selected using AMPure beads (Beckman Coulter) to make sure small RNAs were maximized in the libraries for sequencing (Fig. 1-5A). We applied an iterative alignment strategy (Yuan et al., 2016). The sequences were first mapped to miRBase, unmapped sequences were then mapped to piRNABank, and reads that still couldn't be mapped were mapped to the whole genome (Fig. 1-6A). Of the uniquely mapped small RNAs, piRNAs were the most abundant type in both EVs and donor cells, comprising 35% and 36% of reads respectively. 16% of reads from EVs were mapped to miRNA compared to 26% of reads from donor cells. 24% of reads from EVs were mapped to protein coding regions compared to only 5% of reads from donor cells (Fig. 1-6B).

Considering that miRNAs are the best studied small RNAs, we performed more detailed analysis on miRNAs. Principle component analysis (PCA) for all aligned miRNAs showed that EVs and cells were clearly separated (Fig. 1-6C). Differential expression analysis of miRNAs identified 109 miRNAs that were significantly differentially represented in EVs compared to donor cells, of which 49 were more enriched in EVs. The miRNAs with large fold changes ($Log_2FC>2$ or <-2) were plotted in a heatmap (Fig. 1-6D). In this list, some miRNAs, such as miR-150 (Log_2FC (EV:Cell)=5.59) and miR-320 (Log_2FC (EV:Cell)=2.06), have been reported to be preferentially sorted into EVs in multiple cell types and tissues (Guduric-Fuchs et al., 2012; Zhang et al., 2015). On the contrary, miRNAs such as miR-214 and miR-155, which have been reported to be enriched specifically in EVs from tumor cells were not enriched in our neuronal EVs (Taylor and Gercel-Taylor, 2008; Zhang et al., 2015). Among the miRNAs that were enriched in neuronal EVs, miR-145 (Log_2FC (EV:Cell)=4.58), miR-130b (Log_2FC (EV:Cell)=3.71), miR-296 (Log_2FC

23

(EV:Cell)=2.58), miR-320 (Log$_2$FC (EV:Cell)=2.06) and miR-93 (Log$_2$FC (EV:Cell)=1.73) have all been reported to play critical roles in neuronal development and neurite growth (Chen et al., 2016; Gong et al., 2013; Jauhari et al., 2018; White and Giffard, 2012; Zhang et al., 2016). In conclusion, the population of small RNAs inside neuronal EVs differ significantly from those in donor cells and also from small RNAs detected in EVs from other cell types.

Discussion

In this study, we purified EVs from rat primary neuronal cultures, tested EV transfer between cells, and characterized the population of RNA cargos inside neuronal EVs. Most neuronal EV studies today have focused on specific EV proteins or EV RNAs. Our study revealed a comprehensive map of RNAs inside neuronal EVs and provided multiple miRNA targets for future investigation.

Because of the novelty of our study, we encountered multiple technical challenges. For instance, although we successfully demonstrated that EVs were secreted by donor cells and taken up by recipient neurons in primary neuronal cultures, our system did not mimic the *in vivo* condition well because we incubated recipient cells with very high concentration of EVs. We expended significant effort to validate the EV transfer. In one set of experiments, we incubated recipient cells with medium from CD63-HA-GFP transfected donor cell culture, without purification and concentration of EVs. However, we failed to observe any uptake of CD63-HA-GFP in recipient cells. Following up on a published study using a transwell co-culture system to allow for contact-free co-culture and intercellular EV transfer (Frühbeis et al., 2013), we used a transwell system to co-culture PKH26 labeled or CD63-HA-GFP transfected donor

N2a cells and recipient N2a cells. However, we failed to observe any EV uptake in the recipient

cells. The reason why medium transfer and transwell culture failed might be due to insufficient

EV concentration for detectable uptake. We have also considered direct co-culture, which could

allow us to observe local EV transfer, but this was technically challenging because we would not

be able to distinguish between donor and recipient cells.

We used rat instead of mouse in our study because it was easier to culture rat primary

neurons at large scale. However, this created issues for sequencing data analysis. The rat

genome is not as well annotated as mouse, and rat miRNA databases are not as complete as

mouse, which affected sequencing alignment rate. We tried direct mapping to the rat genome,

which was problematic because many small RNAs such as miRNAs and piRNAs were mapped to

multiple loci on the genome. Thus, we applied an iterative alignment strategy (Yuan et al.,

2016). Functional analysis of miRNAs is challenging because many miRNAs have been reported

but their function has not yet been well characterized. Furthermore, pathway analysis tools

used for mRNAs do not yet exist for miRNAs.

We identified 109 miRNAs that were differentially expressed in EVs compared to donor

cells, 49 of these miRNAs being enriched in EVs. Analysis of the miRNAs that were most

enriched in neuronal EVs revealed that several of them are involved in neuronal development

and neurite growth, which is consistent with previous findings that EVs regulated neurogenesis

and circuit assembly (Liu et al., 2015; Sharma et al., 2019). It will be interesting to test whether

the miRNAs that we identified are transferred and functional in recipient neurons.

We focused our analysis primarily on miRNAs, but piRNAs were actually the most

abundant population in EVs and donor cells. piRNAs are 24-31 nt long and function in

transcriptional regulation of transposable elements in the germline (Weick and Miska, 2014).

piRNAs also play roles outside the germline (Ishizu et al., 2012). Interestingly, it has been

reported that piRNA facilitates DNA methylation to regulate synaptic plasticity in Aplysia

(Rajasethupathy et al., 2012). These findings suggest that it would be interesting to identify

piRNAs that are enriched in neuronal EVs. Finally, the percentage of reads mapped to protein

coding regions in EVs was high (Fig. 1-6B), suggesting that it would be valuable to further

characterize this population of RNAs and to determine whether they are differentially enriched

in EVs compared to donor cells.

   In summary, we successfully purified neuronal EVs and demonstrated that these EVs

were taken up by recipient neurons through endocytosis. We found that the EV miRNA profile

was distinct from the cellular miRNA profile and we identified several miRNAs that were

enriched in neuronal EVs, many of which have been shown to be involved in neuronal

development and neurite growth. In future experiments, we are also interested in determining

whether neuronal EV release and RNA sorting is activity-dependent and whether EV-mediated

transfer of RNAs contributes to synaptic plasticity. The identification of RNAs that are

differentially represented in EVs isolated from stimulated neurons provides a tool for future

studies to elucidate the function of neuronal EVs.

Figures
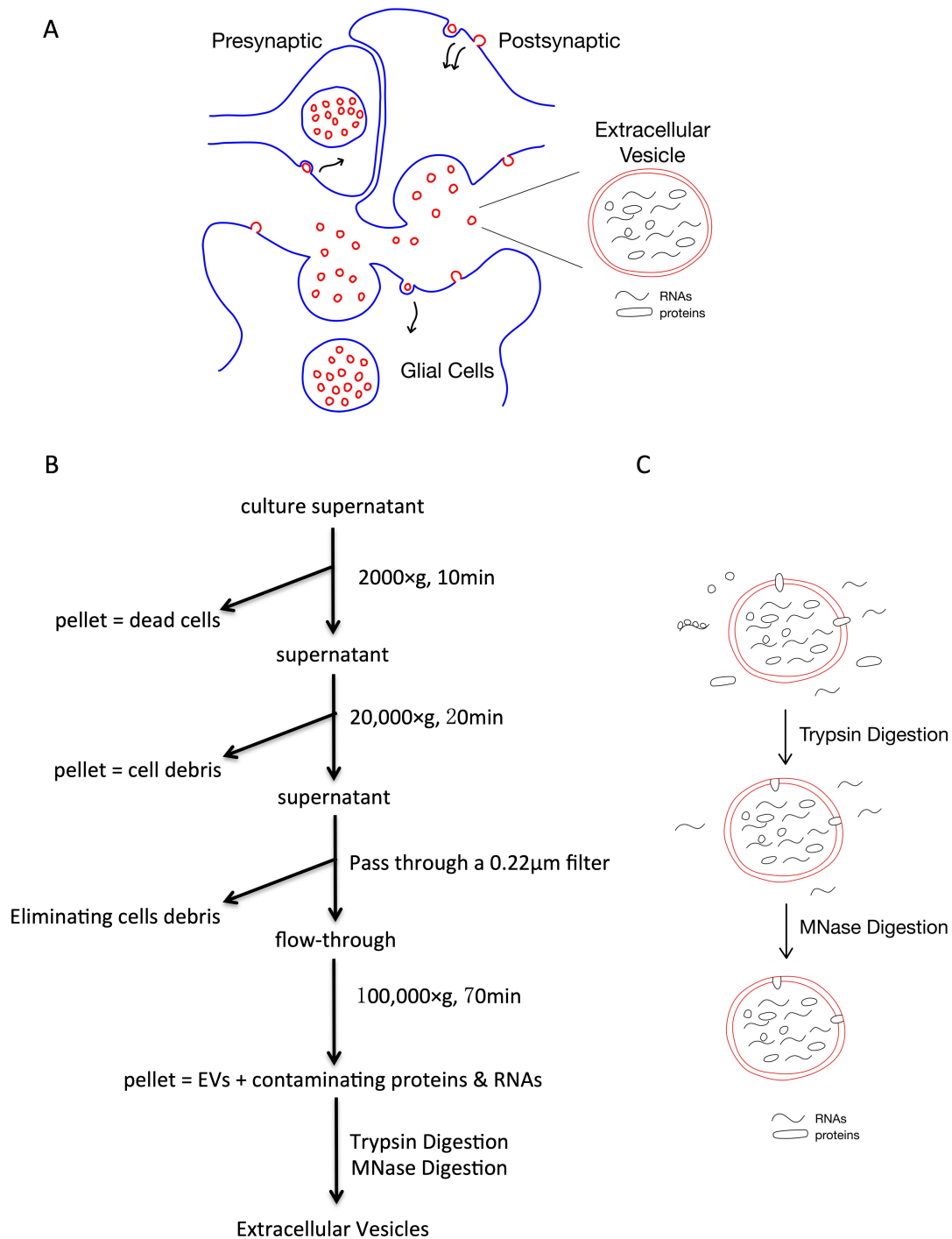
Figure 1-1: Illustration of EV transfer in the nervous system and EV purification protocol. (A) Hypothesis of EV transfer in the nervous system, specifically at the distal synapses. (B) EV purification protocol using ultracentrifugation. (C) Illustration the effect of trypsin and MNase treatment.
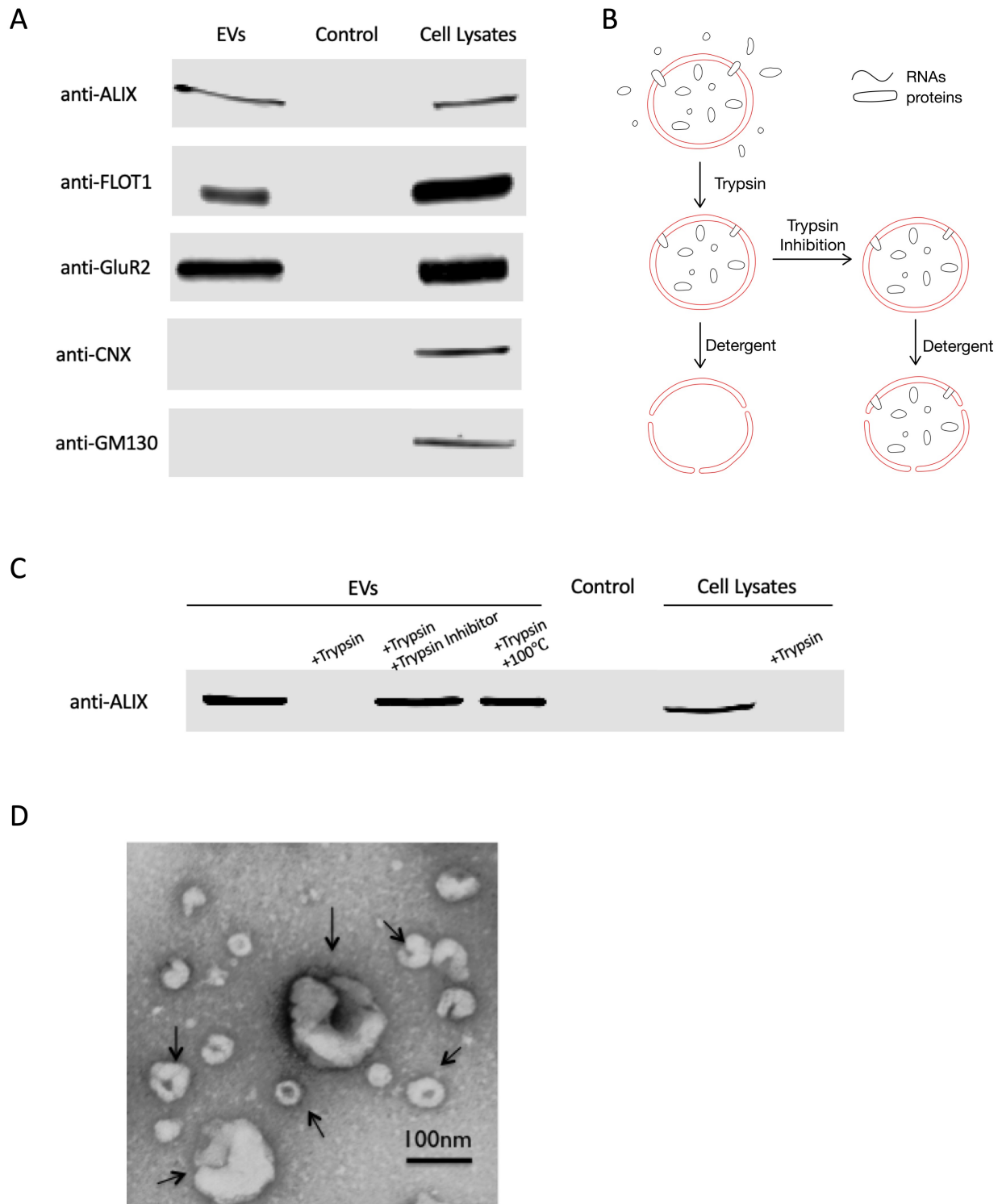
Figure 1-2: EVs are secreted by neurons. (A) Immunoblot of neuronal extracellular vesicles (EVs), pellet of fresh culture medium (Control), and donor cell lysates (Cell Lysates). EVs and cell lysates were prepared from DIV16 cultures, and the same volume of samples (40μL) was loaded

in each lane. (B) Illustration of the trypsin digestion test. EVs were treated with 0.25% trypsin for 15 min at 37℃, then they were either were treated with detergent directly, or trypsin was deactivated first by trypsin inhibitor (5μg/μL) or high temperature (100℃ for 10min) before lysis. (C) ALIX proteins in EVs are protected from trypsin digestion by the surrounding EV membrane. Same volume of samples (EVs or cell lysates from DIV16 cultures) were treated as indicated. (D) EM micrograph of EVs purified from DIV16 cultures. Arrows indicate EVs of various sizes. Scale bar=100nm.
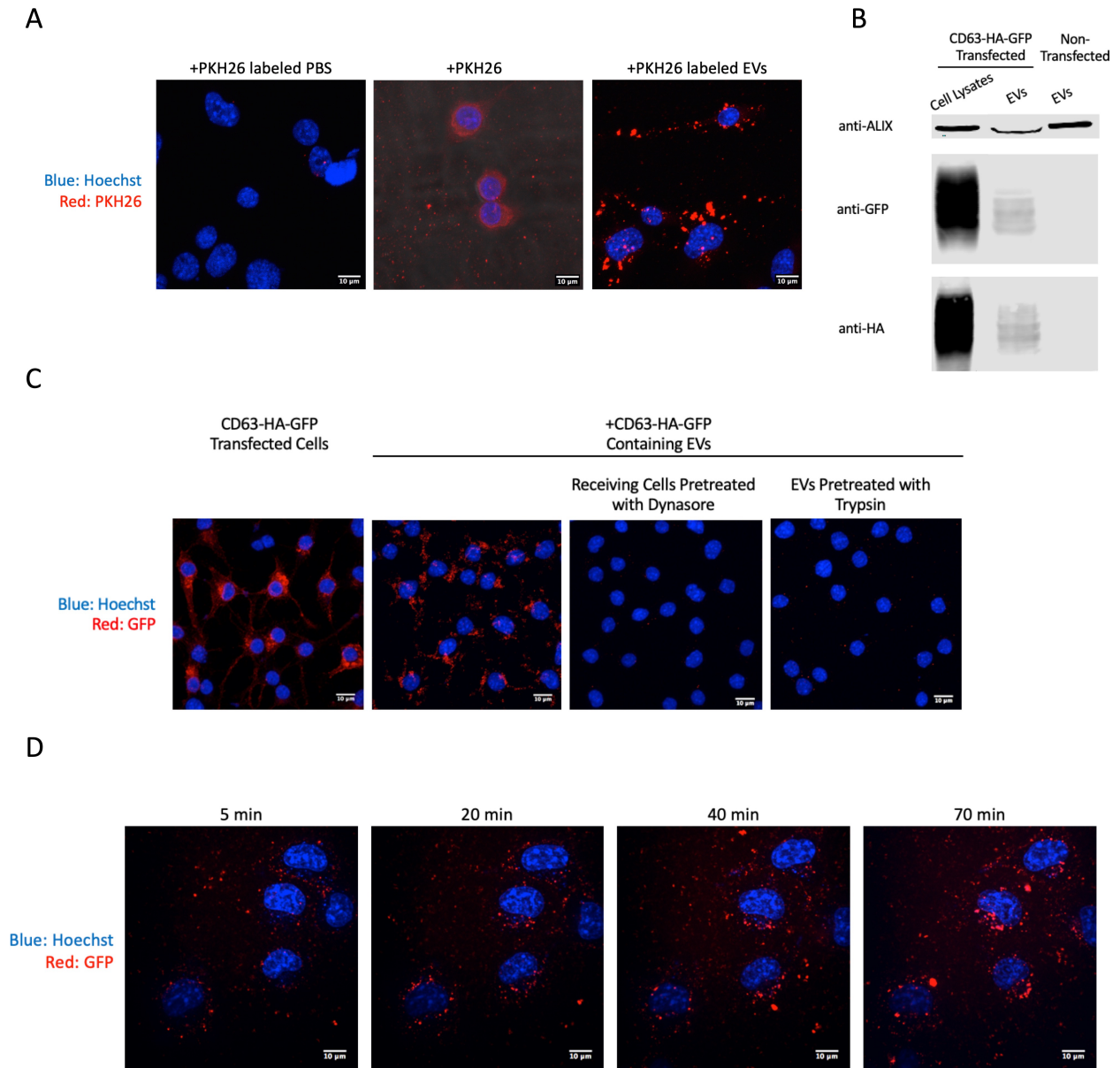
Figure 1-3: EVs are transferred between N2a Cells. (A) PKH26 labeled EVs are taken up by recipient cells. N2a EVs or PBS were labeled with PKH26, then N2a cells were incubated with labeled EVs or PBS for 2 hours. (B) Immunoblot analysis shows CD63-HA-GFP is sorted into EVs. N2a cells were transfected with CD63-HA-GFP and EVs were purified. (C) CD63-HA-GFP is transferred to recipient cells. Pre-treatment of recipient cells with endocytosis inhibitor dynasore or pre-treatment of EVs with trypsin block the uptake of CD63-HA-GFP containing EVs. (D) EVs uptake dynamics. Live imaging of N2a cells incubated with CD63-HA-GFP containing EVs using a spinning disk confocal microscope.

+PKH26 Labeled EVs

Receiving Cells Pretreated
with Dynasore
+PKH26 Labeled EVs

Green: Map2
Blue: Hoechst
Red: PKH26
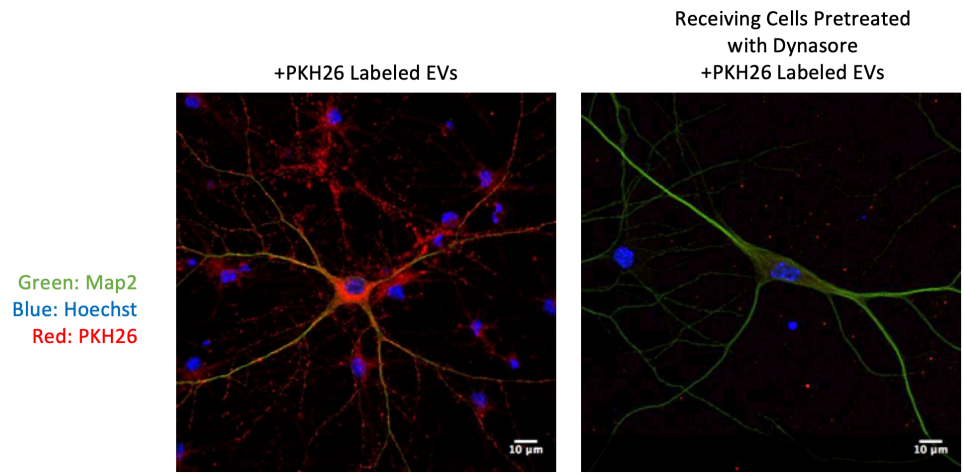
Figure 1-4: EVs are taken up by cultured neurons and glial cells through endocytosis. EVs purified from DIV 16 rat cortical neuronal cultures were labeled with PKH26, then recipient DIV 16 cultures were incubated with labeled EVs for 2 hours. Pre-treatment of recipient cells with the endocytosis inhibitor dynasore blocked the uptake.

A

D16 Neuronal EVs
(After trypsin and
MNase Treatment)

BioAnalyzer Analysis ← Total RNA Isolation → TaqMan Small RNA Assay

ScreenTape Analysis ← Small RNA Library Prep

AMpure Beads Size Selection

Small RNA Sequencing

B

Total RNAs

Small RNAs

Cells

EVs
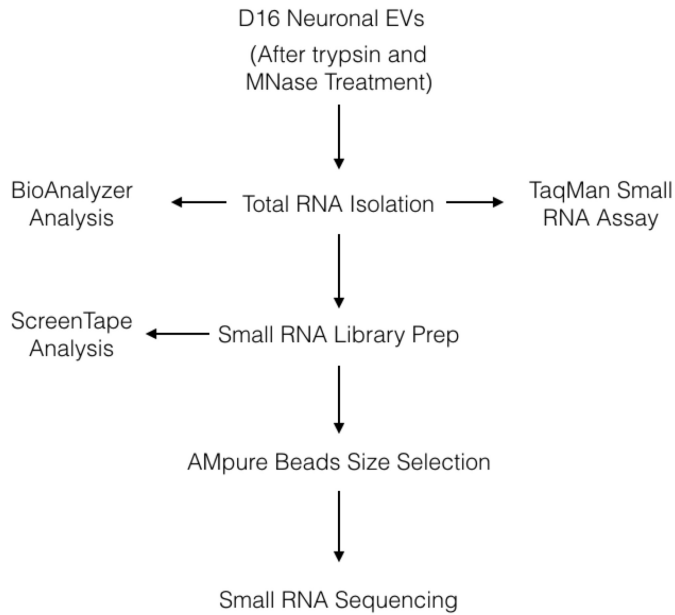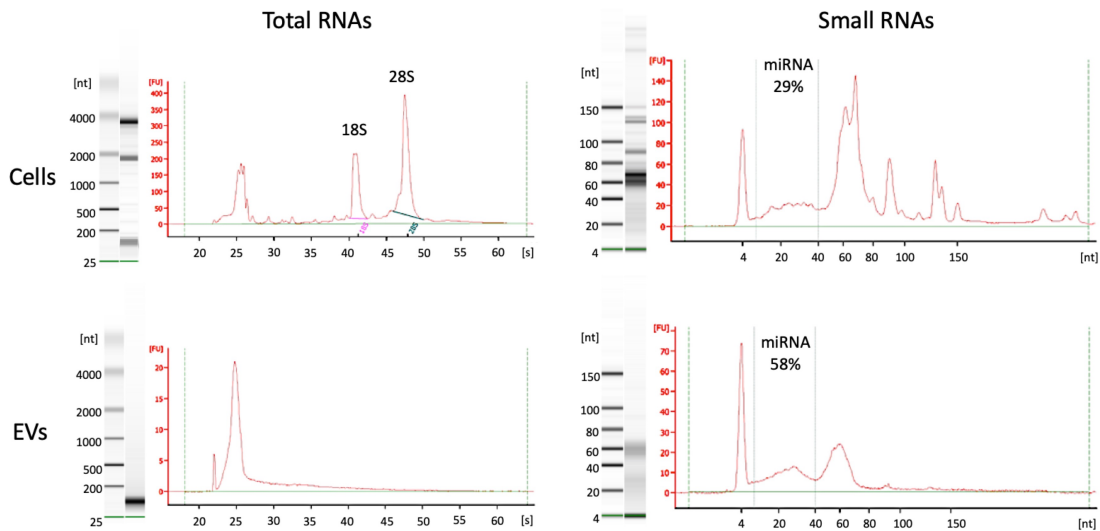
Figure 1-5: Small RNAs are enriched in neuronal EVs. (A) RNA purification and small RNA library preparation protocol (B) Bioanalyzer analysis of the total RNAs (2 peak files on the left) and small RNAs (2 peak files on the right) from DIV 16 neuronal cultures (2 peak files on the top) and corresponding neuronal EVs (2 peak files on the bottom). In the small RNA peak files, the two lines at 10nt and 40nt indicate the range of microRNAs.
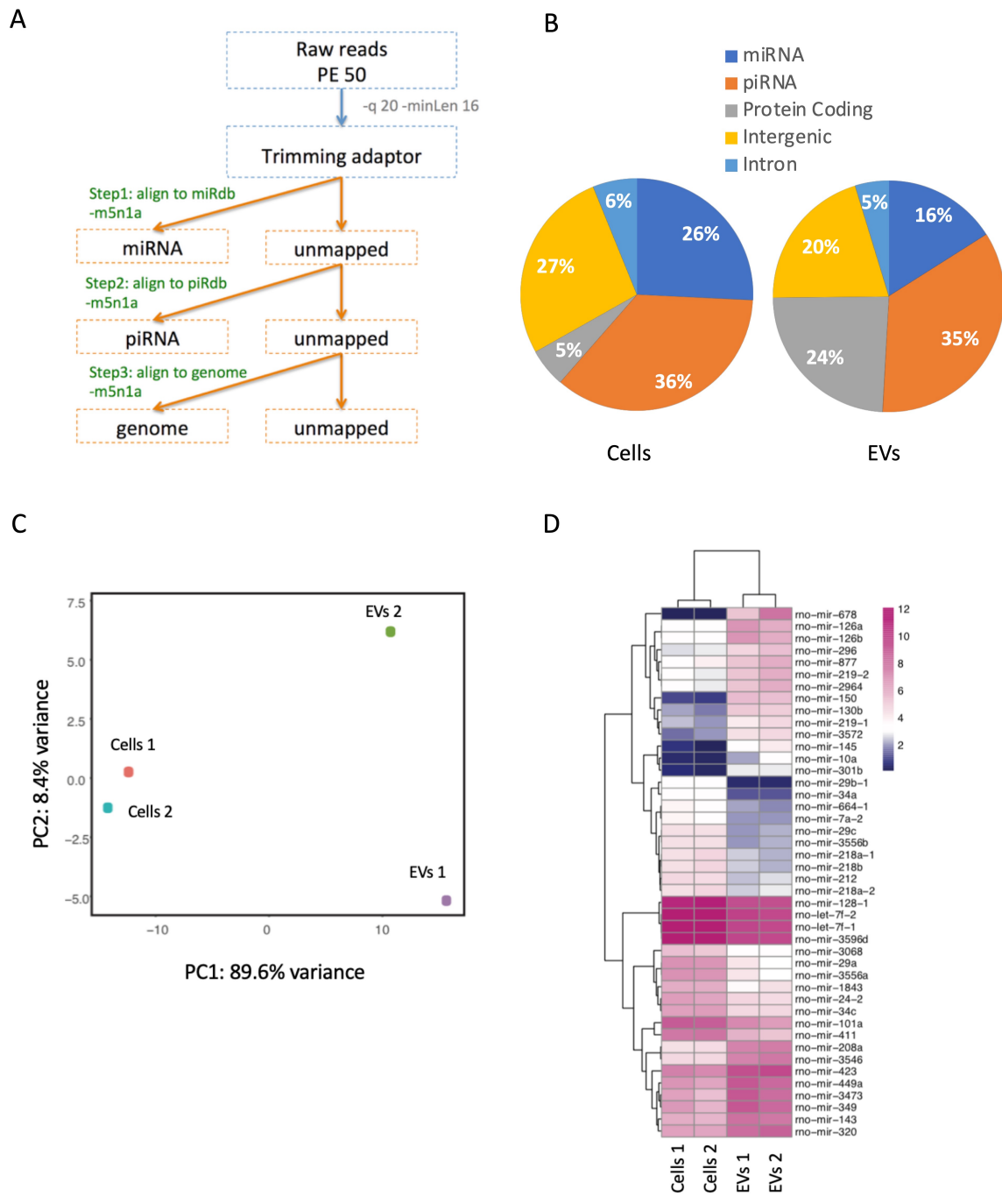
Figure 1-6: miRNAs in neuronal EVs are distinct from those in donor cells. (A) Small RNA sequencing data analysis pipeline. (B) Annotation of uniquely mapped reads in EVs and donor cells. (C) Principle component analysis (PCA) of all the aligned miRNAs. (D) Heatmap of the differentially represented miRNAs (FDR<0.05, Log$_2$FC>2 or <-2).

CHAPTER 3 – Aging Alters the Landscape of Chromatin Accessibility and Pattern of Gene Expression in the Hippocampus

Abstract

Memory loss is a common symptom of aging, ranging from normal age-related cognitive impairment to Alzheimer's disease and other dementias. Changes in neuronal gene expression have been shown to occur with aging in memory centers of the brain(Burke and Barnes, 2006), however the mechanisms by which aging alters gene expression to impact long-term memory remain unclear. To investigate this question, we compared the chromatin accessibility landscape and gene expression pattern of young and aged mouse hippocampus using ATAC-seq and RNA-seq. We found that aging resulted in significant changes in the expression of genes in the hippocampus involved in neurogenesis, immune response, and cell adhesion, as well as in the alternative splicing of some myelin sheath genes. To investigate how sex impacts age-related changes in the hippocampus, we included both female and male mice in our study, and found that aged female mice showed higher expression of some myelin sheath genes compared to aged male mice. Chromatin accessibility analysis revealed a more open chromatin structure in the hippocampus of aged animals compared to young animals, and many of these changes occurred at repetitive elements. However, changes in chromatin accessibility were not well-correlated with changes in gene expression. Our results provide insights into the changes in gene expression that occur with aging, especially genes important for myelin sheath maintenance, and suggest that age-related chromatin accessibility changes may have an indirect role in age-related changes in gene expression.

Introduction

Normal aging often involves some degree of memory impairment, with 40% of the population over the age of 60 years reporting memory problems (HÄNNINEN et al., 1996). Many aspects of brain change with aging including cognitive decline, brain atrophy, blood brain barrier breakdown, activation of the immune system, decreased neurogenesis, altered synaptic connectivity and gene expression changes (Barrientos et al., 2015; Encinas et al., 2011; Fjell et al., 2009; Harada et al., 2013; Shankar et al., 1998; Soreq et al., 2017). Long-term memory requires gene expression for its persistence (Ho et al., 2011), and differences in gene regulation during aging may be central to understanding age-related decline in memory. Genes associated with inflammation have been reported to be upregulated and several genes important for memory differ in their expression in the aging brain (Burke and Barnes, 2006). For instance, the immediate early genes *Arc* and *Narp* were found to be downregulated in the hippocampus of aged rats (Blalock et al., 2003; Penner et al., 2011). Dysregulation of RNA splicing, especially in genes associated with Alzheimer's disease, has also been reported to occur with aging in human and mouse brain (Mazin et al., 2013; Raj et al., 2018; Stilling et al., 2014). However, genome-wide age-related changes in gene expression, alternative splicing, and the regulatory mechanisms underlying any identified differences have not been systematically studied.

Although men and women exhibit differences in age-dependent cognitive decline, brain dystrophy and risk for Alzheimer's disease (León et al., 2016; McCarrey et al., 2016; Pruessner et al., 2001; Viña and Lloret, 2010; Wang et al., 2018), little work has been done to determine whether and how age-related changes in gene expression differ between males and females.

35

Understanding how males and females differ at the level of gene expression may help explain sex-dependent differences during aging, and thereby aid in the development of target therapies for age-related memory disorders.

Dynamic changes in chromatin accessibility are critical to the precise control of gene expression patterns (Su et al., 2017). A recently developed high-throughput method to profile chromatin accessibility, the Assay for Transposases-Accessible Chromatin sequencing (ATAC-seq, Buenrostro et al., 2015) has been used to uncover highly dynamic and global changes in chromatin accessibility during neurogenesis (De La Torre-Ubieta et al., 2018) and neuronal activation (Su et al., 2017). However, to our knowledge, the landscape of chromatin accessibility during brain aging has not been studied. Investigating this landscape has the potential to reveal transcription factor binding sites and gene regulatory networks that are critical for learning and memory.

To this end, we performed RNA-seq and ATAC-seq on the hippocampus from young (10 weeks) and aged (80 weeks) mice, including male and female animals for both age groups. We found that aging was accompanied by widespread changes in gene expression in the hippocampus, including changes in the expression of genes involved in immune response, nervous system development and cell adhesion. Additionally, some genes important for the myelin sheath showed age-dependent alternative splicing and sex-dependent expression differences. We found that aging was associated with higher chromatin accessibility, especially in repetitive elements. These chromatin structure changes, however, were not correlated with transcriptional changes, indicating that age-dependent chromatin opening was not directly related to transcriptional changes.

Materials and Methods

Animals

Young (8 weeks) and aged (78 weeks) male and female C57B16/J mice were purchased from Jackson Laboratories. Use of mice in this study followed the recommendation of and protocol approved by the UCLA Institutional Animal Care and Use Committee. Mice were housed in groups under a 12:12 hr light/dark cycle with food provided ad libitum until they reached the desired ages (10 weeks and 80 weeks). For sample collection, mice were deeply anesthetized with isoflurane before killing by cervical dislocation. The brain was quickly removed and cooled for one minute in ice-cold PBS before the hippocampus from each hemisphere was dissected on ice and processed immediately. For sequencing experiments, one hippocampus was homogenized in Trizol for RNA preparation and the other hippocampus was homogenized for nuclei preparation for ATAC-seq. For qPCR and western blot validation, hippocampal tissue was homogenized in Trizol or RIPA buffer, respectively (see below).

RNA-seq Library Preparation and Sequencing

RNAs were extracted from Trizol using a Trizol/RNeasy hybrid protocol. Briefly, after phase separation, the aqueous phase was mixed with 1 volume of 70% ethanol and passed through a RNeasy spin column (QIAGEN RNeasy Mini Kit). RNA quality was determined using the High Sensitivity RNA ScreenTape Assay (Agilent 5067-5579) and all samples had RIN scores > 7.0. 16 mice were used for differential expression library preparation and 16 mice for splicing library preparation, each including 4 young males, 4 aged males, 4 young females, and 4 aged

37

females. For differential expression analysis, total RNA libraries were prepared using the TruSeq Stranded Total RNA Library Prep Kit with Ribozero (Illumina 20020596). Paired-end 100 bp sequencing to a depth of ~50 million reads per sample was performed using the Illumina HiSeq 2500 system at the UCLA Broad Stem Cell Research Center Sequencing Core. For splicing analysis, mRNA libraries were prepared using the TruSeq Stranded mRNA Library Prep Kit (Illumina 20020594) and paired-end 75 bp sequencing to a depth of ~50 million reads per sample was performed using the Illumina HiSeq2500 system at the UCLA Neuroscience Genomics Core.

ATAC-seq Library Preparation and Sequencing

ATAC-seq sample preparation was performed according to detailed protocols obtained from Hongjun Song's Lab (University of Pennylvania, Buenrostro et al., 2015; Su et al., 2017). Briefly, one hippocampus was homogenized with a Dounce tissue grinder (Wheaton 357544) in 2mL HB buffer (1 mM DTT, 0.15 mM spermine, 0.5 mM spermidine, protease inhibitor (Sigma-Aldrich 04693159001), 0.3% IGEPAL-630, 0.25 M sucrose, 25 mM $MgCl_2$, 20 mM Tricine-KOH). The homogenate was then filtered through a 40 μm strainer. The filtrate was centrifuged over 1 volume of cushion buffer (0.5 mM $MgCl_2$, 0.5 mM DTT, protease inhibitor, 0.88 M sucrose) at 2800 g for 10 minutes in a swinging bucket centrifuge at 4°C. The nuclei pelleted was then resuspended in 20 μL PBS. 1 μL of the nuclei sample was stained with Hoechst to calculate nuclei concentration, and 50,000 nuclei per sample were used for downstream library preparation. Libraries were prepared using the Nextera DNA Library Prep kit (Illumina FC-121-1030) and the quality was analyzed using the D1000 ScreenTape Assay (Agilent 5067-5582).

Paired-end 50 bp sequencing to a depth of ~40 million reads per sample was performed using

Illumina HiSeq 2500 system at the UCLA Broad Stem Cell Research Center Sequencing Core.

RNA-seq Data Analysis

RNA-seq reads from 16 samples (4 young males, 4 aged males, 4 young females, and 4

aged females) were mapped to the mouse genome (mm10) using STAR with the two-pass

option (Dobin et al., 2013). Only uniquely mapped reads were used for the downstream

analysis. Lowly expressed genes were removed by retaining only genes with counts per

million > 0.1 in at least 4 samples (17,823 genes). Read counts were normalized via the trimmed

mean method before differential expression analysis (DEA) (Robinson and Oshlack, 2010). For

DEA, the analysis package edgeR (Robinson et al., 2010) was used, with a FDR < 0.05 cutoff. For

age-dependent expression differences, data from female and male samples were analyzed

separately. For differential splicing analysis, the analysis package rMATS version 4.0.2 (Shen et

al., 2014) was used. At least 5 skipping junction reads in each sample were required for each

splicing event. Five main alternative splicing types results were generated from the rMATS. For

age-dependent splicing differences, data from female and male samples were analyzed

separately. For gene ontology enrichment analysis, the online tool DAVID (Database for

Annotation, Visualization and Integrated Discovery) was used (Huang et al., 2009a, 2009b).

ATAC-seq Data Analysis

ATAC-seq reads from 32 samples (8 young males, 8 aged males, 8 young females, and 8

aged females) were mapped to mouse genome (mm10) using Burrows-Wheeler Aligner (with

parameter setting -a 2000) (Li and Durbin, 2009). Peaks were called on each individual sample using MACS2 (with parameter setting -nomodel -shift 75, Zhang et al., 2008). Peak regions from all samples were integrated to have the same start and end locations. We included peaks that had a read count of ≥ 3 in at least 8 samples and blacklist regions (Amemiya et al., 2019; Consortium, 2012) were removed. Reads in each peak were then counted for each sample using featureCount (Liao et al., 2014). ComBat (Johnson et al., 2007) was used to remove batch effect and differential analysis was performed using DESeq2 (default setting, Love et al., 2014). Peak annotation was done using HOMER (Heinz et al., 2010).

qPCR

Separate biological samples (4 young males, 4 aged males, 4 young females, and 4 aged females) were used for qPCR validation. 50 ng of total RNA was reverse transcribed into cDNA using SuperScript III First Strand Synthesis System (Invitrogen 18080051) with random hexamer primers. Technical triplicates were prepared for each primer set using SYBR Green PCR Master Mix (Applied Biosystems 4309155). The following primers were used:

*Gapdh (F: AGGTCGGTGTGAACGGATTTG; R: TGTAGACCATGTAGTTGAGGTCA),

*Gfap (F: CCCTGGCTCGTGTGGATTT; R: GACCGATACCACTCCTCTGTC),

*Pcdhb9 (F: ACTGCTCTTGAGAATACCAGAGA; R: AGGACGTGAAAATAAGGGTTGG),

Gpr17 (F: TCACAGCTTACCTGCTTCCC; R: CCGTTCATCTTGTGGCTCTTG),

*Ptpro (F: AACATCCTGCCGTATGACTTTAG; R: GGGACTTCTGTTGTAGGACCATC),

*Npnt (F: GGACAGGTCCGATGTCAGTG; R: CTTCCAGTCGCACATTCATCA),

*Dcx (F: CATTTTGACGAACGAGACAAAGC; R: TGGAAGTCCATTCATCCGTGA),

*Tfrc (F: GTTTCTGCCAGCCCCTTATTAT; R: GCAAGGAAAGGATATGCAGCA),

*Mag (F: CTGCCGCTGTTTTGGATAATGA; R: CATCGGGGAAGTCGAAACGG),

*Mbp (F: GACCATCCAAGAAGACCCCAC; R: GCCATAATGGGTAGTTCTCGTGT),

*Cldn11 (F: CTGCCGAAAAATGGACGAACT; R: CTGCACGTAGCCTGGAAGG),

*Mog (F: TCATGCAGCTATGCAGGACAA; R: TTTCGGTAGAGGTGAACCACT).

LINE1 (F: TGAGTGGAACACAACTTCTGC; R: CAGGCAAGCTCTCTTCTTGC),

LINE1.1 (F: ATGGCGAAAGGCAAACGTAAG; R: ATTTTCGGTTGTGTTGGGGTG),

LINE1 5'UTR (F: CTGCCTTGCAAGAAGAGAGC; R: AGTGCTGCGTTCTGATGATG).

Gene primers from PrimerBank (http://pga.mgh.harvard.edu/primerbank/) are indicated with a

*. Primers for LINE1 were obtained from previous publications (De Cecco et al., 2013; Van

Meter et al., 2014). The rest of the gene primers were custom-designed to span exon-exon

junctions. Before comparing between conditions, each Ct value was normalized to the Ct of

GAPDH. The samples were run on the Bio-Rad CFX Connect Real-Time PCR Detection System

and data was analyzed using Excel.

Western Blot

Each hippocampus (16 samples: 4 young males, 4 aged males, 4 young females, and 4

aged females) was homogenized in RIPA buffer with protease and phosphatase inhibitors and

centrifuged at 10,000 g for 10 min at 4°C to remove the cell debris. Protein concentration was

determined using the Pierce BCA Protein Assay Kit (Thermo Fisher 23225). All protein samples

were diluted to 0.5 mg/mL. 4X sample loading buffer (0.2 M Tris-HCl pH 6.5, 4.3 M glycerol,

8.0% (w/v) SDS, 6 mM bromophenol blue, 0.4 M DTT) was added and the samples were boiled

at 95-100°C for 10 min. The samples were then aliquoted and stored at -20°C. Equal amounts of

samples (10-40 mg depending on each protein of interest) were loaded on NuPAGE 4-12% Bis-

Tris protein gels (Invitrogen NP0335BOX) and transferred onto 0.2 μm nitrocellulose

membranes. After transfer, blots were blocked with Odyssey TBS blocking buffer (LI-COR 927-

50000) for 1 hr at room temperature before being incubated in primary antibody at 4°C

overnight. The following primary antibodies were used: anti-TFRC (Invitrogen, 12-6800), anti-

DCX (Abcam, ab18723), and anti-MBP (Abcam, ab218011). The blots were then incubated in

secondary antibodies for 2 hr at room temperature. The blots were imaged using the LI-COR

Odyssey imaging system and quantified using the LI-COR Image Studio software.

Results

To investigate sex- and age- related gene expression, alternative splicing and chromatin

accessibility changes in mouse hippocampus, we dissected the hippocampus from each

hemisphere of young (10 weeks) or aged (80 weeks) mice of both sexes, and used one

hippocampus for RNA-seq and one hippocampus for ATAC-seq library preparation (Fig. 2-1A).

Principle component analysis of the RNA-seq data showed that samples were well-separated by

sex and age by the first and second principle component, respectively (Fig. 2-1B). Overall, 906

genes were differentially expressed either by sex or age, with the largest number of differences

occurring with aging irrespective of sex (Fig. 2-1C). In the hippocampus of females, we found

381 genes were upregulated and 245 genes were downregulated with aging. There were

significantly fewer aging-associated changes in the hippocampus of males compared to females

(chi-square test, p<0.001, X^2 = 93.4). In the hippocampus of males, 178 genes were upregulated

and 153 genes were downregulated with aging (Fig. 2-1D). These results suggest that there are

widespread gene expression changes with aging, including both upregulation and

downregulation of genes, with more genes changing with aging in the hippocampus of females

compared to males.

There is higher expression of myelin sheath-related genes in the hippocampus of aged

females compared to aged males

To investigate how sex differences in gene expression change with aging, we examined

the genes that were differentially expressed between the hippocampus of males and females in

young and aged mice. In the hippocampus of young animals, we found 16 genes that were

differentially expressed between males and females, with 5 genes downregulated and 11 genes

upregulated in females (Fig. 2-2A). In the hippocampus of aged animals, we found significantly

more genes were differentially expressed between the sexes, with 12 genes downregulated and

24 genes upregulated in females. (chi-square test, p = 0.006, X^2 = 7.7; Fig. 2-2A). We found 11 of

the sex-associated differential genes were differentially expressed in both young and aged

mouse (Fig 2-2B), reflecting the fact that most of the sex-associated differences in gene

expression in young animals persisted with aging, and that there was a net increase in number

of genes that showed sex differences with aging. Of the 11 genes that were differentially

expressed between sexes in both young and aged, 9 were on sex chromosomes and 2 were on

chromosome 13 (*Prl*, *Cplx2*). Prolactin (*Prl*), a protein known to be involved in synaptogenesis,

synaptic plasticity and neuroprotection in the hippocampus (Carretero et al., 2019; Torner,

2016), was expressed at a higher level in females than in males in both age groups (young:

Log$_2$FC=4.06, aged: Log$_2$FC=8.06). Complexin 2 (*Cplx2*), a protein involved in synaptic vesicle

fusion (Brose, 2008; Hass et al., 2015), was expressed at a lower level in females than in males

in both age groups (young: Log$_2$FC=-0.16, aged: Log$_2$FC=-0.21). These results indicate that there

may be age-independent differences in plasticity and synaptic vesicle release in the female

versus male hippocampus, and that there is more divergence in the pattern of gene expression

in the hippocampus between males and females with aging.

To further explore the sex differences in gene expression that arise with aging, we

performed gene ontology enrichment analysis on the 25 genes differentially expressed

between female and male hippocampus only in aged animals. We found that myelin sheath

genes were significantly enriched (6 genes: *Mag*, *Mal*, *Mbp*, *Cldn11*, *Cntn2*, *Mog*). These genes

were all expressed at a higher level in the hippocampus of aged females versus aged males (Fig.

2-2C). To test that these differences were indeed due to the upregulation of myelin sheath

genes in females compared to males and not due to a difference in numbers of

oligodendrocytes, we examined the expression level of three oligodendrocyte marker genes

(*Olig1*, *Oli2*, *Opalin*) and found that none were differentially expressed between aged female

and aged male hippocampus (Fig. 2-2C, shading). We also performed qPCR and verified that the

expression of myelin sheath genes *Mag*, *Mbp*, *Cldn11*, and *Mog* were upregulated in the

hippocampus of aged females compared to aged males (Fig. 2-2D). This differential expression

of myelin sheath genes between sexes suggests that females may have less myelin

degeneration or better myelination than males in the hippocampus with aging.

Widespread changes in the expression of genes involved in cell adhesion, immune function and neuronal development are associated with aging

Next, we focused on the sex-independent gene expression changes in the hippocampus with aging. We found that a total of 137 genes were upregulated and 65 genes were downregulated with aging in both sexes (Fig. 2-3A). Gene ontology analysis of these gens revealed that upregulated genes were enriched for genes involved in cell adhesion and immune response, whereas downregulated genes were enriched for genes involved in nervous system development and neuron migration (Fig. 2-3B). We ranked the differentially expressed genes by FDR corrected p-values and found that of the top 10 upregulated and downregulated genes (Fig. 2-3C), 9 (*C4b*, *Abca8a*, *Gfap*, *Il33*, *Ptpro*, *Sox11*, *Dcx*, *Tfrc*, *Gpx8*) have been previously reported to undergo similar age-related changes in the brain (Carlock et al., 2017; Kohman et al., 2011; Qiu et al., 2016; Rowe et al., 2007; Stilling et al., 2014; Uddin and Singh, 2013), whereas others, like the protocadherin genes, have not previously been shown to change with aging.

Protocadherin proteins are calcium-dependent cell-cell adhesion molecules (CAMs) that are critical for correct axonal projections and synapse formation (Chen and Maniatis, 2013; Yagi, 2012). We found that 4 out of the top 10 upregulated genes were protocadherin genes (*Pcdhb2*, *Pcdhb6*, *Pcdhb9*, *Pcdhga6*) (Fig. 2-3C), and protocadherin genes made up the majority of genes in the class "homophilic cell adhesion" which we found to be enriched when we performed gene ontology enrichment analysis (*Cdh23*, *Pcdhb1*, *Pcdhb2*, *Pcdhb3*, *Pcdhb4*, *Pcdhb5*, *Pcdhb6*, *Pcdhb8*, *Pcdhb9*, *Pcdhb14*, *Pcdhb16*, *Pcdhga2*, *Pcdhga6*) (Fig. 2-3B). For example, with aging we found a 75% increase in males and 93% increase in females in the

protocadherin beta 9 (*Pcdhb9*) transcript by RNA-seq and a 110% increase by qPCR (Fig. 2-3C, D). Of the top 10 downregulated genes, several were known to encode proteins that are located at or interact with the extracellular matrix (ECM) (e.g. *Ptpro*, *Tfrc* and *Npnt*) (Fig. 2-3C). For instance, transferrin receptor (TFRC) is a transmembrane protein that interacts with ECM proteins and modulates AMPA receptor trafficking efficiency and synaptic plasticity (Liu et al., 2016). We found that this gene showed age-related downregulation in gene expression of 35% and 26% decrease in males and females, respectively, by RNA-seq (Fig. 2-3C), a 22% decrease in transcript expression by qPCR (Fig. 2-3D), and a decrease in protein levels of 37% in males and 39% in females (Fig. 2-3E). CAMs and ECM are not only important for maintaining the integrity of synapses but are also important for synaptic plasticity formation (Benson et al., 2000; Dityatev and Schachner, 2003). Therefore, with aging there is an alteration in the expression of cell adhesion molecules and extracellular matrix proteins in the hippocampus, potentially contributing to changes in synapse formation and signaling.

Activation of the immune system is known to occur with aging as well as in neurodegenerative diseases (Barrientos et al., 2015; Hong et al., 2016; Stilling et al., 2014). Consistently, gene ontology analysis of age-related upregulated genes showed an enrichment of genes involved with the innated immune response (*B2m*, *C1qa*, *C1qb*, *C1qc*, *C3*, *C4b*, *Defb1*, *Ly9*, *Naip2*, *Trem2*, *Tyrobp*, *Unc93b1*, *Zc3hav1*) (Fig. 2-3B). Besides, two (*C4b*, *Zc3hav1*) of the top 10 upregulated genes were involved in the immune response. Complement component 4B (*C4b*), which showed the most significant increase in expression with aging, has previously been associated with hippocampal aging (Barrientos et al., 2015; Stilling et al., 2014).

Aging resulted in the downregulation of genes involved in nervous system development (*Dcx*, *Dpysl3*, *Dpysl5*, *Fgf13*, *Gfra2*, *Itm2a*, *Ndnf*, *Rgs9*, *Sox11*), and the partially overlapping category of neuron migration (*Aspm*, *Dcx*, *Fgf13*, *Ndn*, *Ndnf*) (Fig. 2-3B), including 3 of the top 10 downregulated genes (*Dpysl3*, *Sox11*, *Dcx*) (Fig. 2-3C). We found a 32% decrease in male and 31% decrease in female transcript expression of the nervous system development and neuron migration gene doublecortin (*Dcx*) by RNA-seq and 13% decrease by qPCR (Fig. 2-3C, D). At the protein level, we saw a 22% decrease in male and 42% decrease in female DCX protein in the hippocampus of aged animals compared to young animals (Fig. 2-3F). This is consistent with the published reports that there is age-dependent decrease of the number of hippocampal stem and progenitor cells (Encinas et al., 2011).

Cell type deconvolution indicates no substantial changes in major hippocampal cell type proportions with aging

Although the total number of cells and the number of neurons in the hippocampus are reported to remain constant with aging (Burke and Barnes, 2006), there is debate as to whether there are age-related changes in the relative proportions of other cell types (Choi and Won, 2011; Palmer and Ousman, 2018). Thus, as an estimate of the changes in cell type proportions with aging, we compared our aging-dependent differential genes with published cell type-specific gene expression data of adult mouse/human brain (McKenzie et al., 2018). We calculated how many of the top 100 most enriched and specific genes for astrocytes, endothelial cells, microglia, neurons and oligodendrocytes from McKenzie et al., 2018 were differentially expressed during aging in our data set. As shown in Table 2-1, a small proportion

of the top 100 cell type-specific genes were differentially expressed with aging: 5 astrocyte-specific genes, 3 endothelial cell-specific genes, 4 neuron-specific genes, 15 microglial-specific genes and 9 oligodendrocyte-specific genes were differentially expressed in the hippocampus of aged versus young animals. Of the 15 microglial genes, all were upregulated in aged animals, and except for *Plek*, the other 14 genes were all known to be associated with microglial activation during neuroinflammation which is known to occur during aging (Castillo et al., 2017; Satoh et al., 2016; Shaftel et al., 2008). Of the 9 oligodendrocyte genes, all were upregulated in aged animals, and 6 (*Ermn*, *Apod*, *Anln*, *Plekhb1*, *S100b*, *Fgfr2*) were known to be related to oligodendrocyte activation and myelination (Aaker et al., 2016; Santos et al., 2018). Thus, the increased expression of these microglial genes and oligodendrocyte genes may not reflect an increase in cell number, but rather may be related to the increased activation of these two cell types during aging.

Alternative splicing of myelin sheath-related genes changes with aging

Alternative splicing is a critical and highly regulated process for generating the molecular diversity that leads to differences in cell function and is especially widespread in the brain (Barbosa-Morais et al., 2012). We compared alternative splicing events from the hippocampus of young and aged mice. We investigated five types of alternative splicing events: skipped exon, alternative 5' splice site, alternative 3'splice site, mutually exclusive exons, and retained intron. We focused on sex-independent alternative splicing changes in the hippocampus with aging, and identified four skipped exon events that were significantly different between samples from young and aged animals in both males and females: 1) inclusion of exon 12 in *Mag*, 2) skipping

of in exon 2 in *Mbp*, 3) skipping of exon 10 in *Bcas1*, and 4) skipping of exon 6 in *Rps24* (Fig. 2-4A, B). As mentioned previously, the overall transcript abundance by RNA-seq and qPCR of myelin sheath genes *Mag* and *Mbp* were greater in aged females compared to aged males (Fig. 2-2C, D), however the proportions of exon inclusion for these genes was similar between the sexes. The skipping of exon 2 in *Mbp* with aging was also evident at the protein level, whereas aged animals of both sexes exhibited a loss of a higher-migrating MBP protein species and a gain of a low-migrating MBP species (Fig. 2-4C). These age-related changes in *Mag* and *Mbp* exon skipping are similar to those occur during development as myelination finished (Tropak et al., 1988; Woodruff and Franklin, 1998). In addition to *Mag* and *Mbp*, *Bcas1* is also known to be involved in myelination (Darbelli et al., 2017; Ishimoto et al., 2017), suggesting that aging is associated with changes in the components important for myelination.

Aging results in more open chromatin structure

Since dynamic changes in chromatin accessibility are critical to the precise control of gene expression patterns (Su et al., 2017), we used ATAC-seq to probe for the chromatin accessibility changes during aging in the hippocampus. For each mouse, the hippocampus from one hemisphere was used for RNA-seq library prep and the hippocampus from the other hemisphere was used for ATAC-seq library preparation (Fig. 2-1A). The number and distribution of peaks in each region was similar between groups (Fig. 2-5A). Similar to the results from our RNA-seq analysis, principle component analysis of read counts from ATAC-seq peaks showed that samples were separated by sex and age by the first and second principle component, respectively (Fig. 2-5B). When assessing age-related chromatin accessibility changes, to increase

the statistical power, females are males were combined together and sex was used as a covariance. We identified 256 differential peaks between the hippocampus of aged and young animals, with 235 regions becoming more open and 21 regions becoming more closed with aging (Fig. 2-5C). For example, a 903bp intergenic region in chromosome 13 showed a significant gain of accessibility in the hippocampus of aged animals of both sexes compared to young animals (Fig. 2-5D, top panel). In contrast, an 862bp intronic region in chromosome 9 showed a significant loss of accessibility in the hippocampus of aged animals of both sexes compared to young animals (Fig. 2-5D, bottom panel). 70% of the differential peaks were located in intergenic regions (Fig. 2-5C), whereas only 40% of the total peaks were located in intergenic regions (Fig. 2-5A), indicating that aging-associated changes in chromatin accessibility occurred predominately in non-coding regions.

We ranked the differential ATAC-seq peaks by FDR corrected p-values and found that within the top 20 differential peaks, 11 were located in retrotransposable elements derived sequences and all of these regions showed an opening in structure with aging (Fig. 2-6A). Furthermore, 24% of all differential ATAC-seq peaks (62/256 peaks) were located in in retrotransposable elements derived sequences. However, further investigation into their sequences revealed that most of these elements had evolved to be incapable of retrotransposition, but they could still be transcribed (Rangwala et al., 2009). On the other hand, during normal aging, long interspersed element-1 (LINE1) retrotransposons become more active in mammalian somatic tissues, including the brain (De Cecco et al., 2013; Van Meter et al., 2014). Thus, we performed qPCR for the retrotransposon LINE1 with three different primers and found that LINE1 retrotransposons were more actively transcribed in the hippocampus of

aged animals compared to that of young animals, with an average of 24% increase in LINE1

transcript expression with aging (Fig. 2-6B). These results indicate that with aging, there is

opening of chromatin in retrotransposon-derived sequences as well as an increase in LINE1

transcript abundance, which could alter the cellular transcriptome and increase genome

instability.

To assess sex-dependent differences in chromatin accessibility, we separated the

samples by sex and performed differential peak analysis (excluding data from sex

chromosomes). We identified one region in young and one region in aged animals which both

showed more opening in females compared to males, although the fold changes were quite

small (Fig. 2-6D). This result is consistent with our RNA-seq data which showed the highest

number of significant differences was associated with aging rather than sex.

There is a lack of association between chromatin accessibility and mRNA expression

Although many of the age-related differential peaks are located in intergenic regions,

they could function as regulatory elements such as enhancers for coding regions (Mora et al.,

2016). Furthermore, repetitive elements, such as LINE1 derived sequences, can function as

gene regulatory elements (Feschotte, 2008). Thus, we assessed the relationship between

differential chromatin accessibility and differential gene expression by calculating the Pearson's

correlation coefficient. We found no significant correlation for either aging or sex. Because

enhancers do not always regulate the genes with the nearest TSS (Andersson et al., 2014), this

analysis is limited in correctly identifying a corresponding ATAC-seq peak and gene. Thus, we

manually assessed the ATAC-seq and RNA-seq data on a genome browser, checking ATAC-seq

peaks which were 500 kbp upstream and downstream of the top 20 age-related differentially expressed genes, as well as any genes 500 kbp upstream and downstream of the top 20 age-related differential ATAC-seq peaks. However, we did not identify any correlation between chromatin accessibility changes and gene expression changes. Considering that enhancers can regulate genes more than 500 kbp away, we also checked the chromatin interactions from published Hi-C dataset (Bonev et al., 2017) and looked for domains that interacted with the top differential ATAC-seq peaks. However, we did not find any interactions more than 500 kbp away. Thus, our results suggest chromatin accessibility changes may not have a direct effect on gene expression changes during aging and between sexes.

Discussion

In this study, we performed RNA-seq and ATAC-seq on the hippocampus of young and aged mice of both sexes. Previous studies have tested transcriptional changes during mouse hippocampal aging (Pawlowski et al., 2009; Stilling et al., 2014), but, to our knowledge, this is the first study that also examined chromatin accessibility changes.

Our findings of increased expression of immune response genes is consistent with previous findings (Lucin and Wyss-Coray, 2009). However, it is unknown whether this increase indicates a protective function against aging or if the increase in immune response genes contribute to cognitive impairment during aging. In an Alzheimer's disease mouse model, the innate immune system genes *C1q* and *C3* are upregulated and are thought to mediate synapse loss by activating microglia (Hong et al., 2016) and these genes were also found to be upregulated with aging in our study. Two other genes we found to be upregulated with aging,

52

the microglial immune-related genes *Trem2* and *Tyrobp*, are known to affect amyloid deposits

in an Alzheimer's disease mouse model (Haure-Mirande et al., 2017). On the other hand,

activated microglia could also play a protective role during aging. In a mouse demyelinating

disease model, the innate immune system genes *C1qa*, *C1qb*, *C1qc*, *Tyrobp* and *Trem2*

expression levels are up-regulated in microglia (Elliott et al., 2013). It is known that microglia

support the regeneration of myelin after injury through clearance of debris, secretion of

regeneration factors, and modification of the extracellular matrix (Lloyd and Miron, 2019).

Thus, it is possible that myelin sheath degeneration during aging activates microglia to facilitate

repair.

The decreased expression of nervous system development genes has also been reported

to occur during brain aging. One hypothesis is that the age-related decline in the production of

new neurons contributes to cognitive impairment during aging (Encinas et al., 2011). However,

whether adult neurogenesis exists is still under debate (Boldrini et al., 2018; Sorrells et al.,

2018). Thus, decreased expression of neurogenesis genes may indicate depletion of neuronal

stem cells during aging, but not necessarily decreased neurogenesis.

The changes in ECM and CAMs during aging are not well characterized, although the

ECM and CAMs play critical roles in synapse formation and synaptic plasticity (Chen and

Maniatis, 2013; Dityatev and Schachner, 2003; Yagi, 2012). The change in the expression level

of protocadherin genes during aging had not been previously reported, however there are

known age-related changes in the methylation of CpG sites across protocadherin genes (El Hajj

et al., 2017; Slieker et al., 2016). Such epigenetic changes could be the cause of differential

gene expression. Aside from protocadherin genes, *Ptpro*, *Tfrc*, *Npnt* are all involved in ECM and

were found to be downregulated during aging. Thus, it is possible that dysregulation of ECM and CAMs during aging causes deficits in neuronal connectivity and synaptic plasticity in the hippocampus.

We found that aging had moderate differential effects on the expression of genes in males versus females. A human brain study using exon arrays found widespread gene expression splicing differences between males and females, however the biggest differences occurred in occipital cortex and thalamus. In cerebellum and hippocampus, most of the differences occurred in genes from the X and Y chromosomes but not from autosomes (Trabzuni et al., 2013). This is consistent with our finding of small differences in gene expression and alternative splicing between sexes. Of the 11 genes that were differentially expressed between sexes from the hippocampus of both young and aged animals, 2 genes, *Prl* and *Cplx2*, were on autosomes. In the hippocampus, prolactin functions as a neuropeptide and is related to neurogenesis, neuronal plasticity and neuroprotection (Carretero et al., 2019; Torner, 2016). The sex-dependent difference in Complexin 2 expression has not previously been reported. Complexins regulate neurotransmitter release at synapses and its dysregulation is related to neurodegenerative diseases (Brose, 2008; Hass et al., 2015). Its differential expression between sexes could be related to the gender differences in neurodegenerative diseases prevalence.

We found myelin sheath genes were expressed at a higher level in the hippocampus of aged females compared to that of aged males. The myelin sheath is critical for the integrity of nerve fibers and the conduction of action potentials (Nave and Werner, 2014). During aging, some myelin sheaths undergo degeneration, while new myelin formation and remyelination continues (Peters, 2002; XIE et al., 2014). The higher expression level of myelin sheath-related

genes in the hippocampus of aged female mice could indicate female hippocampal tissue have less myelin degeneration or better remyelination than that in males during aging. An electron microscopy study in 18-month old aged Long-Evans rats found that in aged females, the total volumes of the myelin sheaths were significantly bigger than those in aged males (18 months) (Yang et al., 2008), which is consistent with the findings in our study. Sex-dependent differences in myelin sheath gene expression could contribute to the increased age-associated brain atrophy in males compared to females (Pruessner et al., 2001; Xu et al., 2000). However, whether there are differences in myelin degeneration or myelination in the hippocampus of females versus males with aging requires further investigation. Considering that we were not able to identify sex differences in chromatin accessibility of differentially expressed myelin-related genes, other factors must regulate the differential gene expression between sexes during aging.

The age-dependent splicing differences in the hippocampus we identified during hippocampal aging were smaller than those seen in previous aging studies (Mazin et al., 2013; Stilling et al., 2014). The difference may arise from that fact that we used the splicing analysis software rMATS (Shen et al., 2014) which is able to detect novel splicing events and has higher precision at the expense of sensitivity compared to other packages (Hooper, 2014). The splicing differences we identified included mostly genes involved the myelin sheath pathway. The alternative splicing of the myelin sheath gene *Mag* is tightly regulated during development in the brain: exon 12 skipped isoforms are expressed at higher level than exon 12 included isoforms during active myelin formation through CNS development, however in the adult brain, exon 12 included isoforms predominate (Tropak et al., 1988). Our data show that during aging,

there was a further increase of exon 12 included isoforms and decrease of exon 12 skipped

isoforms, which may suggest there is a decrease in myelination rate during aging. Although it

has been reported that myelination continues with aging (XIE et al., 2014), how the rate

changes is not well studied. Similarly, the alternative splicing of exon 2 in the myelin-related

gene *Mbp* is also known to be regulated during development. The isoforms with exon 2 are

enriched during active myelin formation and their levels decrease as myelination completes

(Woodruff and Franklin, 1998). We show that aging is accompanied by a further decrease of

exon 2-included isoforms, suggesting that the rate of myelination may undergo further

decreases during aging. Less is known about *Bcas1* alternative splicing during development, but

it is reported that the loss of *Bcas1* causes hypomyelination and induces expression of

inflammation-related genes (Ishimoto et al., 2017). The RNA binding protein quaking,

dysregulation of which causes demyelination, is known to regulate alternative splicing of *Mag*,

Mbp and *Bcas1* in oligodendrocytes (Darbelli et al., 2017; Wu et al., 2002). In quaking-deficient

oligodendrocytes, exon 12 included Mag isoforms are overexpressed (Fujita et al., 1990). Thus,

one hypothesis is that during hippocampus aging, quaking regulates the alternative splicing of

Mag, *Mbp* and *Bcas1*, causing a decrease in myelination rate.

This is the first study, to our knowledge, to examine chromatin accessibility changes in

the hippocampus during aging. Our finding that the chromatin structure is more open with

aging is consistent with the "heterochromatin loss model of aging" (Pal and Tyler, 2016;

Tsurumi and Li, 2012; Villeponteau, 1997). This model, first purposed in 1997, suggests that

there is a loss of heterochromatin during aging, leading to alterations in the expression of genes

residing in these regions (Villeponteau, 1997). The strongest evidence is that eukaryote life

span can be shortened or lengthened by modifying heterochromatin structure using histone

deacetylase inhibitors or activators. Histone modification and DNA methylation changes occur

during aging, including but not limited to loss of trimethylation on H3K4, H3K9, H3K27 and

H3K36, increased acetylation on H3K9 and H3K27, and hypermethylation of DNA (Pal and Tyler,

2016). These epigenetic changes could contribute to the differences in chromatin accessibility.

Thus, it would be interesting to look into how epigenetic modifications change in hippocampus

during aging and to compare these data with our ATAC-seq data to identify whether and which

post-translational modifications contribute to the chromatin accessibility changes during

hippocampal aging.

Our results show that most of the age-associated chromatin accessibility changes

occured in intergenic and intronic regions, not at promoter regions. Additionally, many of the

top age-related differential ATAC-seq peaks were in retrotransposons LINE1 derived sequences.

Around 18% of the mouse genome is estimated to be LINE1 derived sequences (Cordaux and

Batzer, 2009), however, during evolution 99.5% of the elements lost their capability of

retrotransposition due to chromosome rearrangement and deletion (Richardson et al., 2015).

Although most of the LINE1 derived sequences we identified to be more open in aged animals

are no longer capable of retrotransposition, they could still be transcribed and their RNAs could

cause cellular inflammation and malfunction (De Cecco et al., 2019; Rangwala et al., 2009).

During aging, there is activation of retrotransposable elements in mammalian somatic tissues

including brain, which was thought to result from loss of heterochromatin (De Cecco et al.,

2013; Van Meter et al., 2014). Histone deacetylase SIRT6 binds to LINE1 retrotransposons and

represses their activity through modulating the heterochromatin status of nearby regions.

During aging, SIRT6 was found to depleted from LINE1, leading to over-expression of LINE1 (Van Meter et al., 2014). Although the LINE1-derived sequences identified in our study are no longer active due to missing elements, they could still be transcribed and their accessibility and transcription could be regulated by histone deacetylases like SIRT6. Thus, it would be interesting to look into how chromatin binding of SIRT6 and other histone deacetylases changes in the hippocampus during aging.

We were not able to identify any correlation between transcriptional changes and chromatin accessibility changes. This finding may not be surprising given a number of factors, including that our assignment of intergenic peaks to nearest genes may not be accurate and that binding of transcriptional repressors can also cause chromatin opening. However, even when we examined the ATAC-seq and RNA-seq browser tracks manually, taking long distance regulations into consideration, we did not identify any obvious relationships. From the perspective of gene transcription, most of the differentially expressed genes were expressed in both aged groups or sex groups although at different levels, which means that their promoter and enhancer regions were likely open in all groups. Thus, the binding of regulators may not further impact their accessibility. From the perspective of chromatin accessibility, chromatin structure at enhancers and promoters needs to be open for active transcription, however open chromatin structure alone is not sufficient to induce transcriptional changes. Other factors, such as binding of transcriptional factors and DNA looping are required as well (Li et al., 2007). To summarize, the chromatin accessibility changes and the gene expression changes may both be results of epigenetic alterations, however we did not find a relationship between them.

In conclusion, this study represents the first description of a comprehensive map of gene expression, splicing and chromatin accessibility changes during aging for both male and female mice. Our finding of altered cell adhesion and myelin sheath genes during aging provide novel targets for both experimental and clinical studies. Finally, our finding of increased chromatin accessibility but lack of correlation with transcriptional changes provides novel starting points for future studies on chromatin structure and gene expression regulation during brain aging.

Figures

A
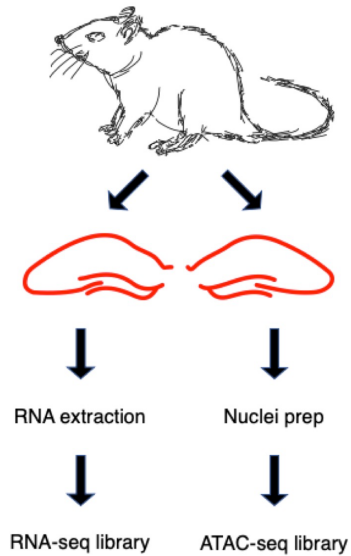
B
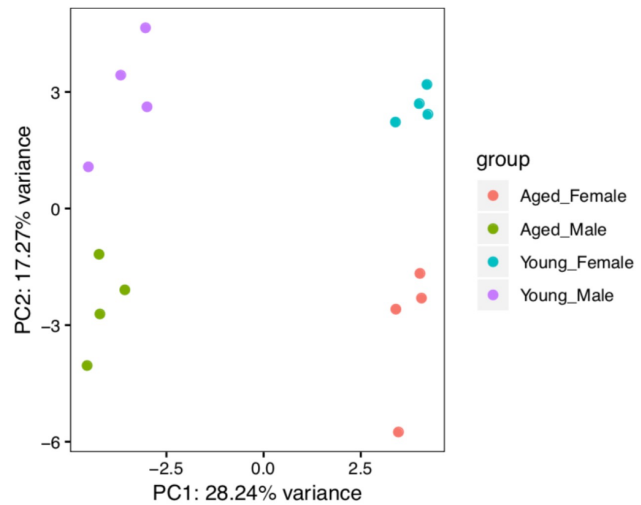
C

D
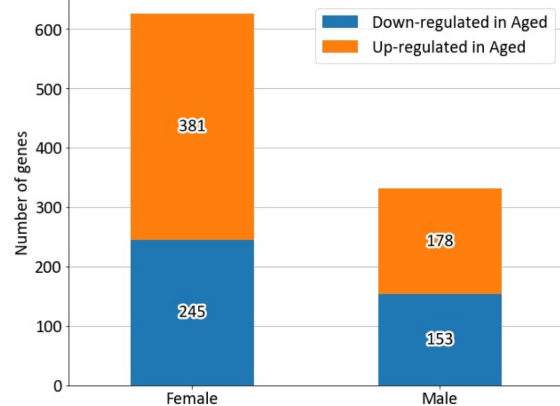
Figure 2-1: Age-related gene expression changes in female and male mouse hippocampus. (A) Illustration of the experiment design. (B) Principle component analysis (PCA) of the RNA-seq gene expression data. (C) Heatmap of 906 sex or age-related differentially expressed genes (FDR < 0.05). Red indicates highly expressed genes; blue indicates lowly expressed genes. (D) Number of genes that are differentially expressed between aged and young animals in female

and male (FDR < 0.05, $Log_2CPM > 0$). n=4 for each group (young female, aged female, young male, aged male).

A

B

C

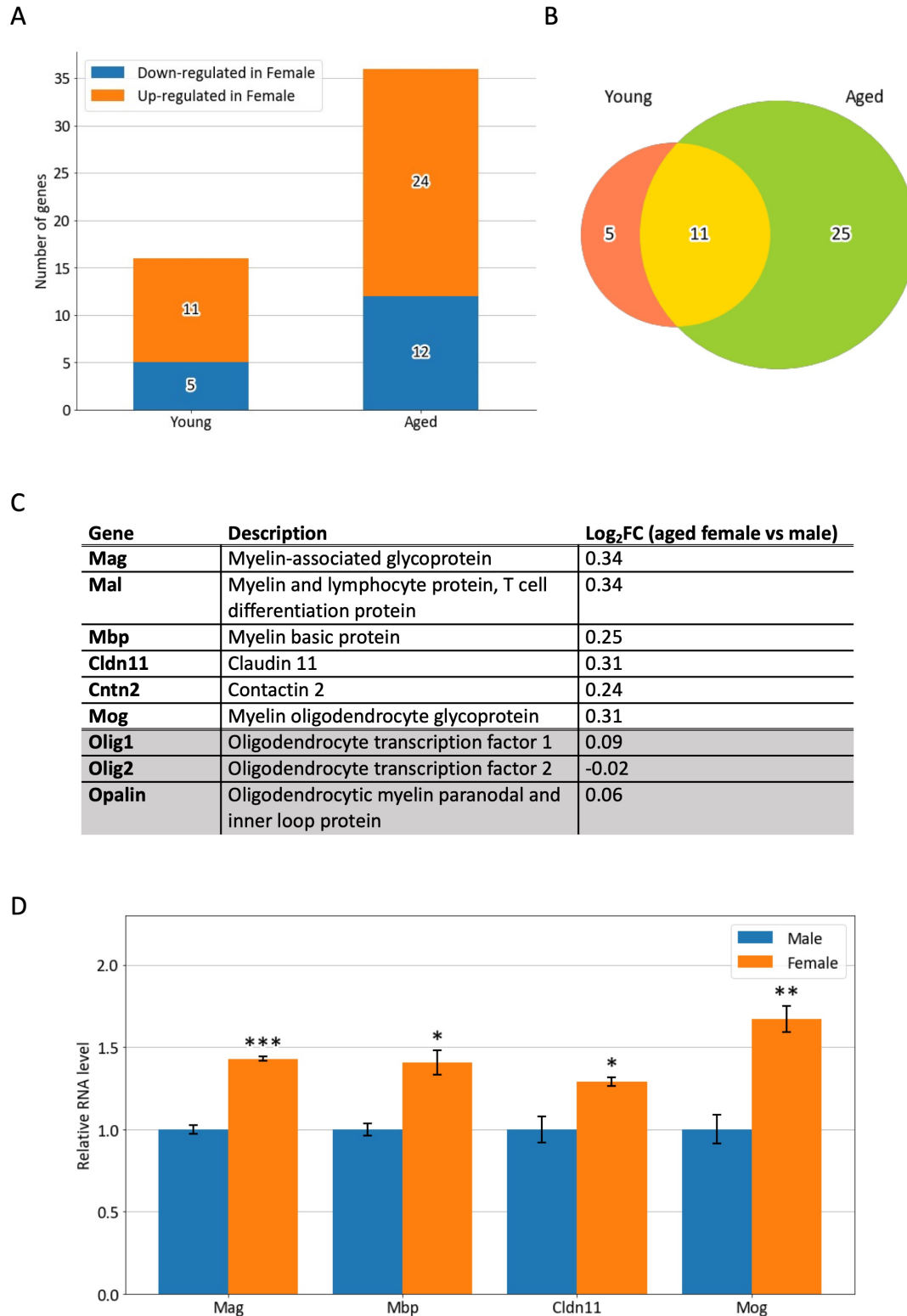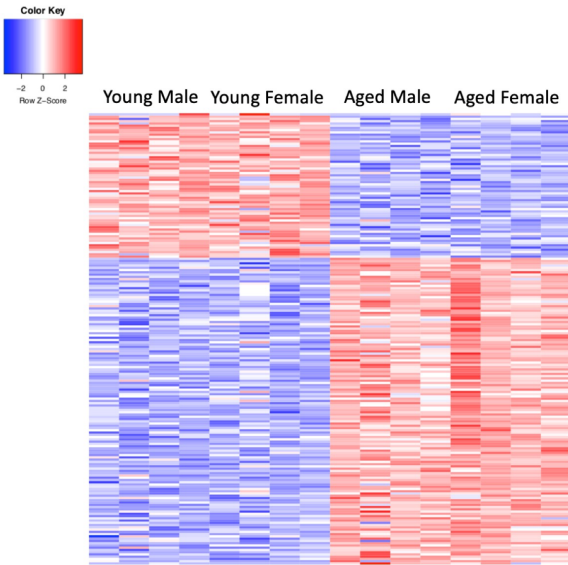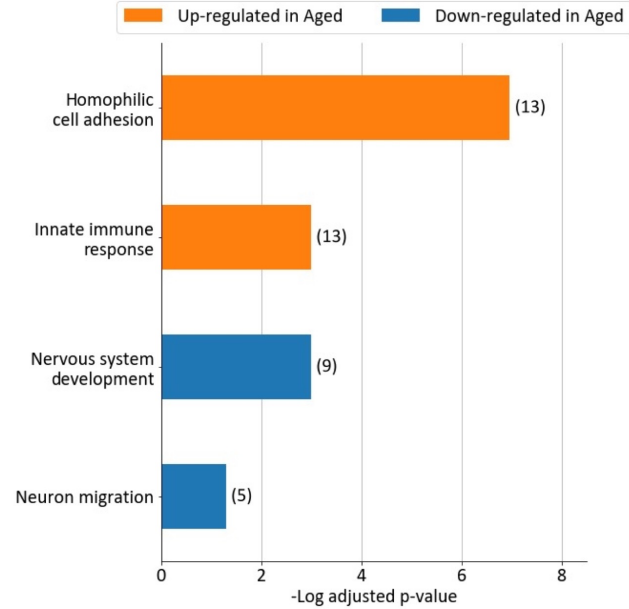| Gene	Description	Log$_2$FC (aged female vs male)
Mag	Myelin-associated glycoprotein	0.34
Mal	Myelin and lymphocyte protein, T cell differentiation protein	0.34
Mbp	Myelin basic protein	0.25
Cldn11	Claudin 11	0.31
Cntn2	Contactin 2	0.24
Mog	Myelin oligodendrocyte glycoprotein	0.31
Olig1	Oligodendrocyte transcription factor 1	0.09
Olig2	Oligodendrocyte transcription factor 2	-0.02
Opalin	Oligodendrocytic myelin paranodal and inner loop protein	0.06

D

Figure 2-2: There is higher expression of myelin sheath-related genes in the hippocampus of aged females compared to aged males. (A) Number of genes that are differentially expressed

between female and male hippocampus in young and aged animals (FDR < 0.05, $Log_2CPM > 0$). (B) Venn diagrams comparing genes that are differentially expressed (FDR < 0.05, $Log_2CPM > 0$) between female and male hippocampus in young and aged groups. (C) List of myelin sheath-related genes that are differentially expressed (FDR < 0.05) between aged male and aged female hippocampus. Shaded rows show oligodendrocyte marker genes, which are not differentially expressed. (D) qPCR validation of myelin sheath genes in aged male and aged female, showing the mean ± s.e.m of transcript abundance, normalized to Gapdh. T-test: *adjusted p < 0.05, ** adjusted p < 0.005, *** adjusted p < 0.0005. n = 4 animals for each condition.

A

Color Key

Row Z-Score
−2 0 2

Young Male | Young Female | Aged Male | Aged Female

B

Up-regulated in Aged | Down-regulated in Aged

Homophilic cell adhesion (13)
Innate immune response (13)
Nervous system development (9)
Neuron migration (5)

-Log adjusted p-value

C

| Gene	Description	Log$_2$FC (aged vs young male)	Log$_2$FC (aged vs young female)
C4b	complement component 4B	1.29	1.75
Pcdhb9	protocadherin beta 9	0.81	0.95
Abca8a	ATP-binding cassette, sub-family A, member 8a	0.78	0.97
Gfap	Glial fibrillary acidic protein	0.49	0.63
Zc3hav1	Zinc finger CCCH type, antiviral 1	0.89	1.13
Pcdhb2	Protocadherin beta 2	1.02	0.93
Pcdhb6	Protocadherin beta 6	1.11	0.99
Il33	Interleukin 33	0.56	0.75
Neat1	Nuclear paraspeckle assembly transcript 1	0.75	0.88
Pcdhga6	Protocadherin gamma subfamily A, 6	0.63	0.59
Ptpro	Protein tyrosine phosphatase, receptor type O	-0.55	-0.49
Gpr17	G protein-coupled receptor 17	-0.73	-0.55
Igfbpl1	Insulin-like growth factor binding protein-like 1	-3.20	-3.01
Tfrc	Transferrin receptor	-0.62	-0.44
Npnt	Nephronectin	-0.60	-0.58
Dpysl3	Dihydropyrimidinase-like 3	-0.31	-0.41
Sox11	SRY-box containing gene 11	-0.41	-0.55
Dcx	Doublecortin	-0.55	-0.53
Gpx8	Glutathione peroxidase 8	-1.22	-1.29
Top2a	Topoisomerase II alpha	-1.24	-1.38

64
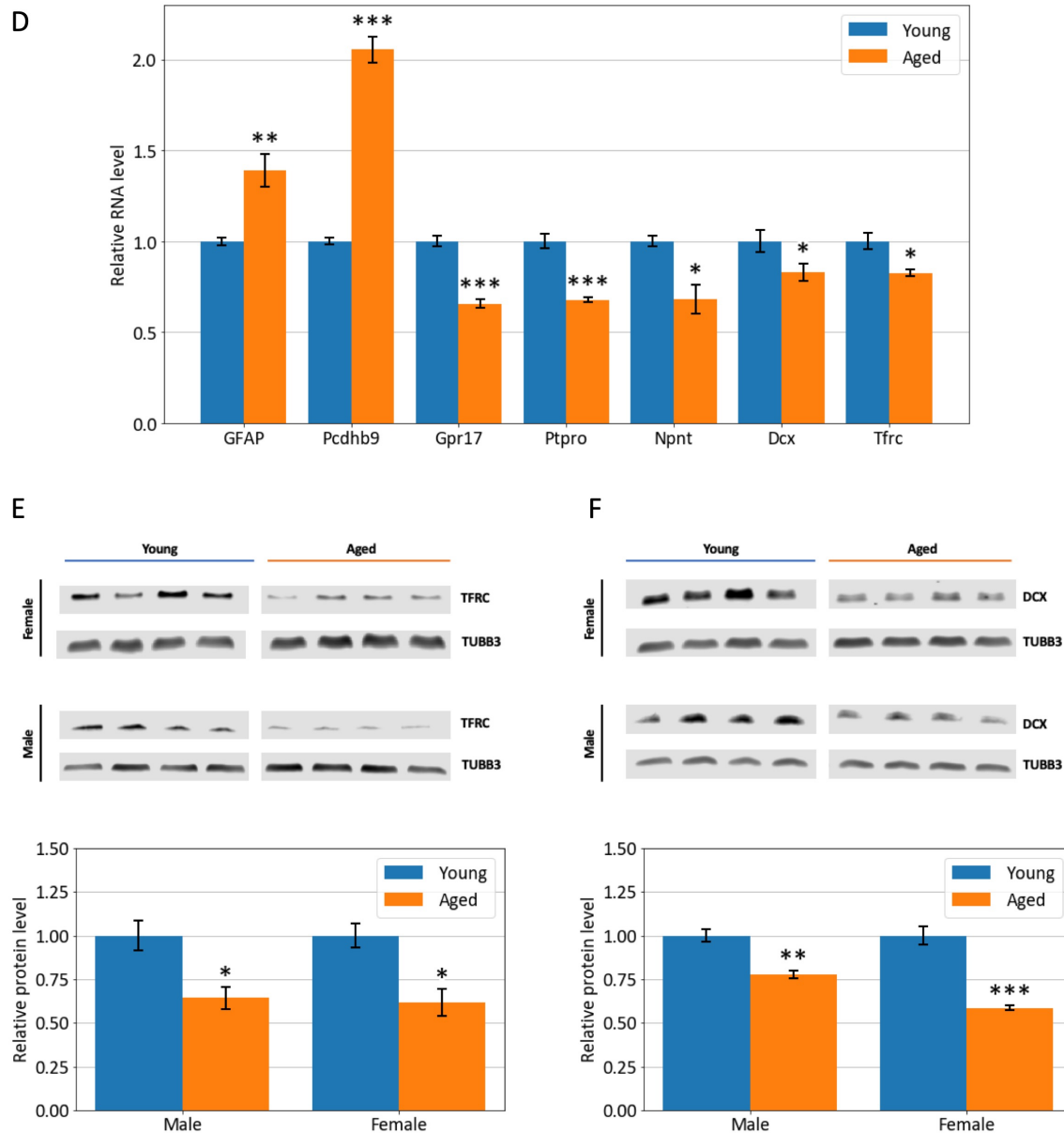
Figure 2-3: Aging is associated with changes in the expression of cell adhesion, immune response and nervous system development genes. (A) Heatmap of 202 age-related differentially expressed genes common to both sexes (FDR < 0.05). Red indicates highly expressed genes; blue indicates lowly expressed genes. (B) Biological pathway analysis of genes that are upregulated (orange) and downregulated (blue) in aged animals. Only categories with adjusted p-value < 0.05 are shown here. The numbers on the right represent the number of DE genes in that category. (C) List of top age-related differential genes that are common between male and female. Genes that are up and down regulated in aged animals are listed separately and each is ranked by FDR corrected p-values. (D) qPCR validation of selected top aging-associated differential genes, showing the mean ± s.e.m of transcript abundance, normalized to

65

Gapdh. T-test: *adjusted p < 0.05, ** adjusted p < 0.005, *** adjusted p < 0.0005. n = 8 animals for each condition (young and aged). (E) Quantitative western blot analysis for TFRC. TUBB3 was used as loading control. Bar graphs on the bottom indicate mean ± s.e.m of TFRC signal normalized to TUBB3. T-test: *adjusted p < 0.05, ** adjusted p < 0.005, *** adjusted p < 0.0005. n = 4 animals for each condition. (F) Quantitative western blot analysis for DCX, presented as in (E).

Cell Type	Gene	Description	Log$_2$FC (aged vs young male)	Log$_2$FC (aged vs young female)
Astrocyte (5)	Chrdl1	chordin-like 1	0.54	0.46
	Gfap	glial fibrillary acidic protein	0.49	0.63
	Ncan	neurocan	-0.30	-0.27
	Slc7a10	solute carrier family 7 (cationic amino acid transporter, y+ system), member 10	-0.25	-0.23
	Il33	interleukin 33	0.56	0.75
Endothelial (3)	Itm2a	integral membrane protein 2A	-0.24	-0.30
	Clic5	chloride intracellular channel 5	0.41	0.38
	Osmr	oncostatin M receptor	0.69	0.70
Microglia (15)	C1qb	complement component 1, q subcomponent, beta polypeptide	0.31	0.51
	Ctss	cathepsin S	0.48	0.69
	Il1a	interleukin 1 alpha	0.98	1.17
	Plek	pleckstrin	0.32	0.49
	CD83	CD83 antigen	0.24	0.48
	Trem2	triggering receptor expressed on myeloid cells 2	0.48	0.75
	Tyrobp	TYRO protein tyrosine kinase binding protein	0.36	0.66
	Selplg	selectin, platelet (p-selectin) ligand	0.32	0.33
	C1qc	complement component 1, q subcomponent, C chain	0.33	0.49
	C1qa	complement component 1, q subcomponent, alpha polypeptide	0.32	0.58
	Mpeg1	macrophage expressed gene 1	0.36	0.52
	Lcp1	lymphocyte cytosolic protein 1	0.33	0.55
	Tmem119	transmembrane protein 119	0.35	0.37
	Pld4	phospholipase D family, member 4	0.45	0.52
	Itgb2	integrin beta 2	0.50	0.69
Neuron (4)	Penk	preproenkephalin	0.31	0.33
	Ndnf	neuron-derived neurotrophic factor	-0.32	-0.31
	Glra2	glycine receptor, alpha 2 subunit	-0.43	-0.42
	Dcx	doublecortin	-0.55	-0.53
Oligodendrocyte (9)	Ermn	ermin, ERM-like protein	0.40	0.44
	Apod	apolipoprotein D	0.38	0.59
	Anln	anillin, actin binding protein	0.51	0.57
	Plekhb1	pleckstrin homology domain containing, family B (evectins) member 1	0.28	0.30
	Evi2a	ecotropic viral integration site 2a	0.41	0.37
	S100b	S100 protein, beta polypeptide, neural	0.34	0.48
	Dock5	dedicator of cytokinesis 5	0.32	0.26
	Pla2g16	phospholipase A2, group XVI	0.34	0.42
	Fgfr2	fibroblast growth factor receptor 2	0.28	0.35

Table 2-1: Comparison of differentially expressed genes with top 100 most enriched and specific genes in astrocyte, endothelial, microglia, neuron and oligodendrocyte cell types.

A

| Gene	Description	Exon Position	Exon Inclusion in Young Female	Exon Inclusion in Aged Female	Exon Inclusion in Young Male	Exon Inclusion in Aged Male
Mag	Myelin-associated glycoprotein	chr7: 30900351-30900396	0.64	0.80	0.58	0.76
Mbp	Myelin basic protein	chr18: 82561777-82561855	0.12	0.10	0.14	0.08
Bcas1	Breast carcinoma-amplified sequence 1	chr2: 170366363-170366528	0.12	0.05	0.13	0.11
Rps24	Ribosomal protein S24	Chr14: 24495429-24495449	0.98	0.95	0.99	0.95

B
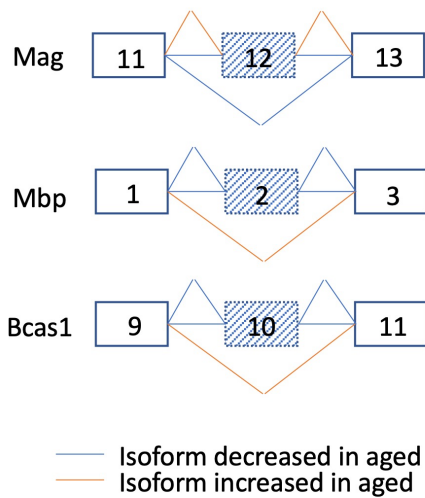
C
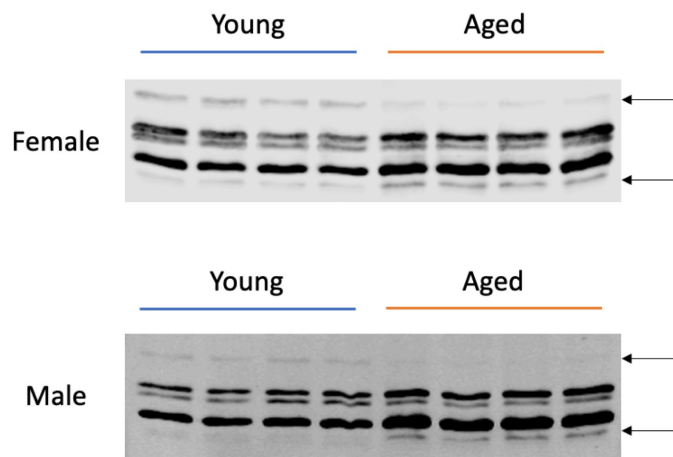
Figure 2-4: Aging is associated with splicing changes in myelin sheath-related genes. (A) List of genes that underwent alternative splicing during aging in both male and female (B) Diagrams showing the alternative splicing events in myelin sheath-related genes *Mag*, *Mbp* and *Bcas1* during aging. (C) Western blot analysis for MBP. Arrows point to the isoforms that are differentially expressed with aging.
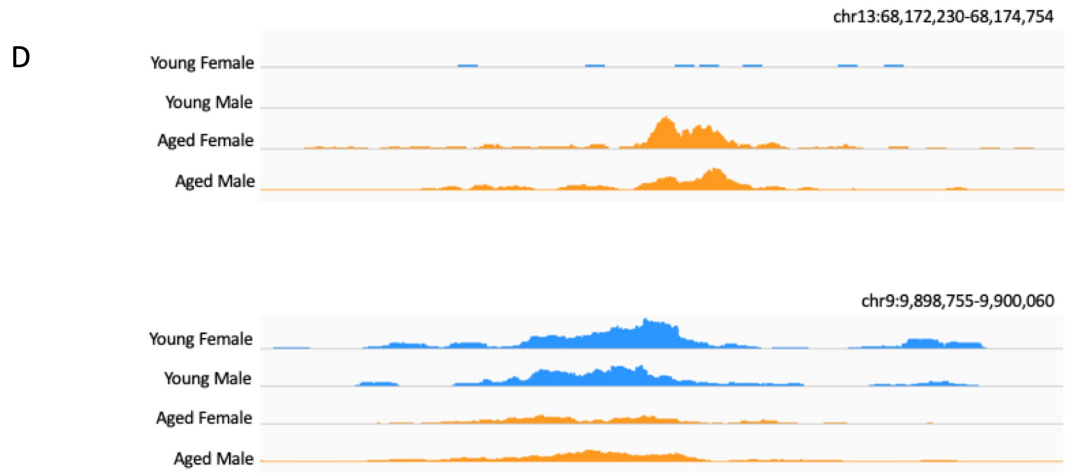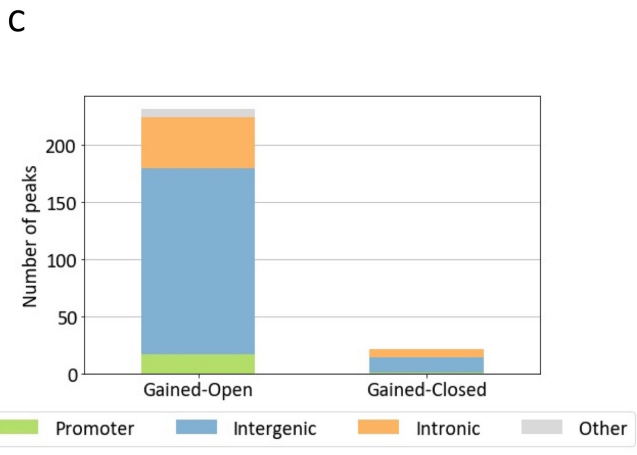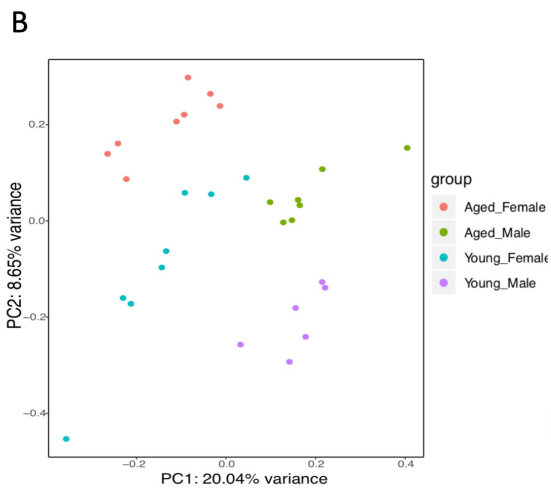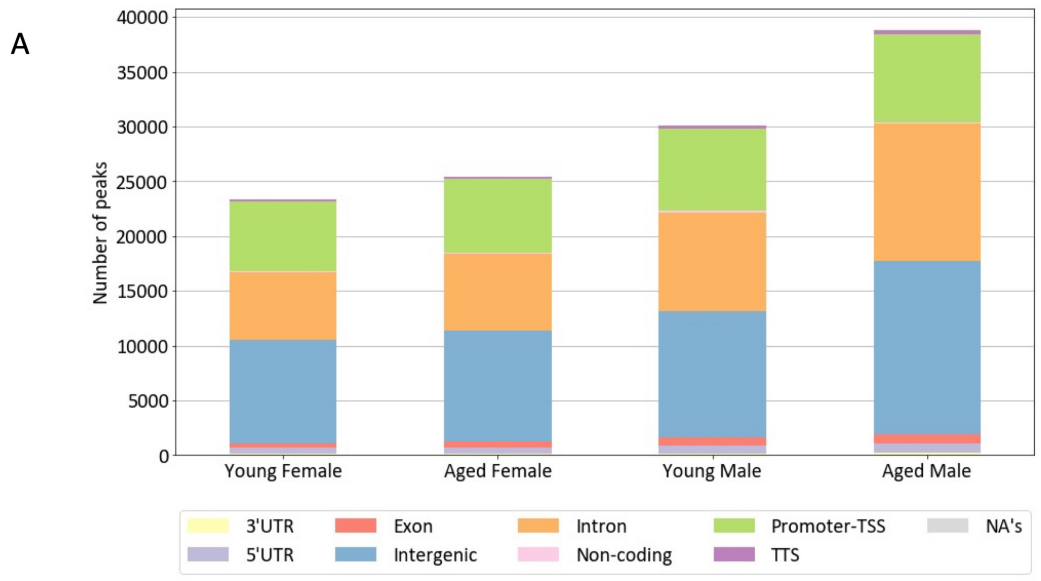
A

B

C

D

chr13:68,172,230-68,174,754

chr9:9,898,755-9,900,060

Figure 2-5: Aging is associated with higher chromatin accessibility, with most of the changes occurring at intergenic regions. (A) Genome annotation of peaks in each condition. The data is from averaging the four biological replicates in each condition in first round of ATAC-seq. (B) Principle component analysis of reads in ATAC-seq peaks. (C) Genome annotation of peaks that are different (FDR < 0.05) between young and aged animals. Regions that have higher accessibility in aged animals are called gained-open; regions that have lower accessibility in aged animals are called gained-closed. (D) Genome browser visualization of example regions that have significantly different chromatin accessibility between young and aged animals. Tracks show reads normalized to total reads number for each sample. Blue tracks indicate data from the hippocampus of young animals and orange tracks indicate data from the hippocampus of aged animals.

A

Region	Log$_2$FC (aged vs young)	Annotation	Distance to TSS
chr13:68173012-68173972	1.81	MuRRS-int|LTR|ERV1	310166
chr12:113424298-113425426	1.40	(CAGCT)n|Simple_repeat	-64703
chr4:122566757-122567454	1.66	G-rich|Low_complexity	-122153
chr4:144454917-144455543	1.59	3' UTR	8526
chr13:68258143-68258746	1.39	MuRRS-int|LTR|ERV1	323659
chr14:42200924-42201665	1.29	L1MA5A|LINE|L1	58753
chr13:3343584-3344063	1.30	Intergenic	-134479
chr14:43025788-43026323	1.16	L1MA6|LINE|L1	-10480
chr14:41499002-41499664	1.16	L1MA5A|LINE|L1	273071
chr13:68116864-68117140	1.14	MuRRS-int|LTR|ERV1	253676
chr14:41656527-41657248	1.13	L1MA5A|LINE|L1	115516
chr14:43357961-43358709	1.04	L1MA5A|LINE|L1	-10524
chr7:15749191-15749702	1.11	promoter-TSS	-923
chr13:68306167-68306598	1.09	Intergenic	275721
chr14:42807995-42808703	1.06	L1MA7|LINE|L1	-10414
chr14:41537664-41538263	1.09	Intergenic	234440
chr14:41667839-41668535	1.02	Intergenic	104217
chr14:43618187-43618731	0.96	L1MA7|LINE|L1	-10446
chr17:39591503-39591967	0.99	Lx5c|LINE|L1	-49222
chr13:68049672-68050069	0.94	Intergenic	186545
chr13:68086299-68087031	0.96	Intergenic	223339

B
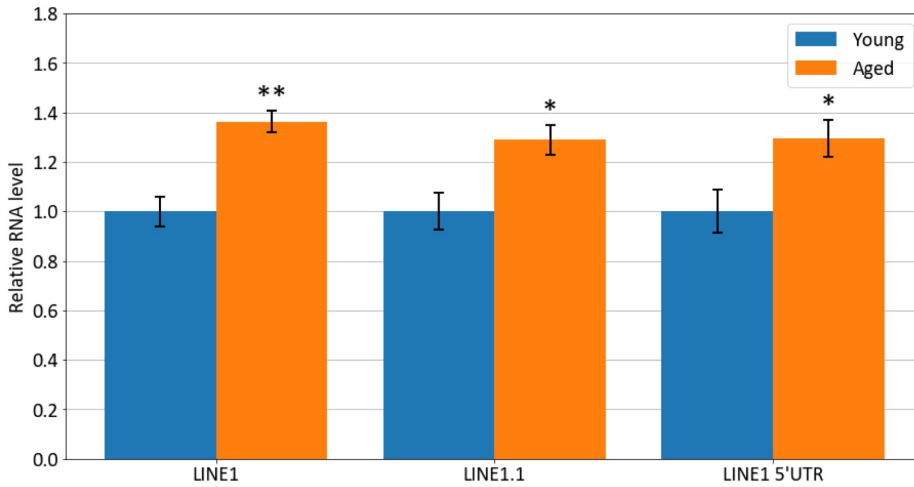
C

Age	Region	logFC (female vs male)	Detailed Annotation	Distance to TSS
Young	chr17:13305888-13306404	0.13	(CTGTG)n|Simple_repeat	-48426
Aged	chr17:13550660-13553248	0.11	(CTGTG)n|Simple_repeat	2140

Figure 2-6: Aging is associated with higher chromatin accessibility in repetitive elements and higher activity of retrotransposable elements. (A) List of top ATAC-seq differential peaks between the hippocampus of young and aged animals, ranked by FDR corrected p-values. (B) qPCR of LINE1 RNA in the hippocampus using 3 different primers for LINE1, showing the mean ±

s.e.m of transcript abundance, normalized to Gapdh. T-test: *adjusted p < 0.05, ** adjusted p < 0.005, *** adjusted p < 0.0005. n = 8 animals for each condition (young and aged). (C) List of ATAC-seq differential peaks between the hippocampus of young and aged females and males.

CHAPTER 4 – CONCLUSIONS

In conclusion, we studied neuronal gene expression during memory from two perspectives, the role of extracellular vesicles and the impact of aging on gene expression in mouse hippocampus.

Memory results from changes in the strength of the synaptic connections between neurons and translation of synaptically localized mRNAs is important for long-term synapse-specific neuronal plasticity. The finding that EVs contain RNAs and that neuronal EV secretion is regulated by synaptic activity leads to the hypothesis that EVs may be transferred between cells in the nervous system and that mRNAs and microRNAs transferred through this pathway contribute to local translation during neuronal plasticity. Most neuronal EV studies so far focused on specific EV proteins or EV RNAs, and have not used genome-wide RNA sequencing approaches to identify the entire population of RNAs present in EVs.

As described in Chapter 2, we demonstrated that EVs were released from rat primary neuronal cultures and were taken up by recipient neurons through endocytosis. We showed that the RNAs inside neuronal EVs were very different from those present in donor cells or from the RNAs that have been detected in EVs from other cell types. Detailed analysis revealed the EV miRNA profile was distinct from the cellular miRNA profile and we found that several miRNAs that were enriched in neuronal EVs are involved in neuronal development and neurite growth. Our study provides a comprehensive map of RNAs inside neuronal EVs and provides multiple miRNA targets for future investigation.

Normal aging often involves some level of memory impairment as such, can be considered a physiological manipulation of plasticity and memory, with the comparison between young and aged mice providing insights into differences in gene regulation that may be central to plasticity and memory. However, genome-wide age-related changes in gene expression, alternative splicing, and the regulatory mechanisms underlying any identified differences have not been systematically studied. In particular, the landscape of chromatin accessibility during brain aging is unknown.

As described in Chapter 3, our data revealed that there were widespread gene expression changes in the hippocampus, including genes involved in immune response, nervous system development and cell adhesion. Additionally, some genes important for the myelin sheath showed age-dependent alternative splicing and sex-dependent expression differences. We found that aging was associated with higher chromatin accessibility, especially in repetitive elements. These chromatin structure changes, however, were not correlated with transcriptional changes, indicating that age-dependent chromatin opening was not directly related to transcriptional changes. This study, to our knowledge, is the first description of a comprehensive map of gene expression, splicing and chromatin accessibility changes during aging for both male and female mice. Our finding of altered cell adhesion and myelin sheath genes during aging provide novel targets for both experimental and clinical studies. Finally, our finding of increased chromatin accessibility but lack of correlation with transcriptional changes provides novel starting points for future studies on chromatin structure and gene expression regulation during brain aging.

REFERENCES

Aaker, J.D., Elbaz, B., Wu, Y., Looney, T.J., Zhang, L., Lahn, B.T., and Popko, B. (2016). Transcriptional Fingerprint of Hypomyelination in Zfp191null and Shiverer (Mbpshi) Mice. ASN Neuro *8*.

Amemiya, H.M., Kundaje, A., and Boyle, A.P. (2019). The ENCODE Blacklist: Identification of Problematic Regions of the Genome. Sci. Rep. *9*, 9354.

Andersson, R., Gebhard, C., Miguel-Escalada, I., Hoof, I., Bornholdt, J., Boyd, M., Chen, Y., Zhao, X., Schmidl, C., Suzuki, T., et al. (2014). An atlas of active enhancers across human cell types and tissues. Nature *507*, 455–461.

Andreae, L.C. (2018). Adult neurogenesis in humans: Dogma overturned, again and again? Sci. Transl. Med. *10*, eaat3893.

Ashley, J., Cordy, B., Lucia, D., Fradkin, L.G., Budnik, V., and Thomson, T. (2018). Retrovirus-like Gag Protein Arc1 Binds RNA and Traffics across Synaptic Boutons. Cell *172*, 262-274.e11.

Ball, M.J. (1977). Neuronal loss, neurofibrillary tangles and granulovacuolar degeneration in the hippocampus with ageing and dementia. A quantitative study. Acta Neuropathol. *37*, 111–118.

Barbosa-Morais, N.L., Irimia, M., Pan, Q., Xiong, H.Y., Gueroussov, S., Lee, L.J., Slobodeniuc, V., Kutter, C., Watt, S., Colak, R., et al. (2012). The Evolutionary Landscape of Alternative Splicing in Vertebrate Species. Science (80-.). *338*, 1587–1593.

Barrientos, R.M., Kitt, M.M., Watkins, L.R., and Maier, S.F. (2015). Neuroinflammation in the normal aging hippocampus. Neuroscience *309*, 84–99.

Beery, A.K., and Zucker, I. (2011). Sex bias in neuroscience and biomedical research. Neurosci. Biobehav. Rev. *35*, 565–572.

Benson, D.L., Schnapp, L.M., Shapiro, L., and Huntley, G.W. (2000). Making memories stick: cell-adhesion molecules in synaptic plasticity. Trends Cell Biol. *10*, 473–482.

Blalock, E.M., Chen, K.-C., Sharrow, K., Herman, J.P., Porter, N.M., Foster, T.C., and Landfield, P.W. (2003). Gene microarrays in hippocampal aging: statistical profiling identifies novel processes correlated with cognitive impairment. J. Neurosci. *23*, 3807–3819.

Boldrini, M., Fulmore, C.A., Tartt, A.N., Simeon, L.R., Pavlova, I., Poposka, V., Rosoklija, G.B., Stankov, A., Arango, V., Dwork, A.J., et al. (2018). Human Hippocampal Neurogenesis Persists throughout Aging. Cell Stem Cell *22*, 589-599.e5.

Bonev, B., Mendelson Cohen, N., Szabo, Q., Fritsch, L., Papadopoulos, G.L., Lubling, Y., Xu, X., Lv, X., Hugnot, J.-P., Tanay, A., et al. (2017). Multiscale 3D Genome Rewiring during Mouse Neural

Development. Cell *171*, 557-572.e24.

Booth, A.M., Fang, Y., Fallon, J.K., Yang, J.-M., Hildreth, J.E.K., and Gould, S.J. (2006). Exosomes and HIV Gag bud from endosome-like domains of the T cell plasma membrane. J. Cell Biol. *172*, 923–935.

Brody, H. (1955). Organization of the cerebral cortex. III. A study of aging in the human cerebral cortex. J. Comp. Neurol. *102*, 511–556.

Brose, N. (2008). For Better or for Worse: Complexins Regulate SNARE Function and Vesicle Fusion. Traffic *9*, 1403–1413.

Buenrostro, J.D., Wu, B., Chang, H.Y., and Greenleaf, W.J. (2015). ATAC-seq: A Method for Assaying Chromatin Accessibility Genome-Wide. Curr. Protoc. Mol. Biol. *109*, 21.29.1-9.

Burke, S.N., and Barnes, C.A. (2006). Neural plasticity in the ageing brain. Nat. Rev. Neurosci. *7*, 30–40.

Carlock, C., Wu, J., Shim, J., Moreno-Gonzalez, I., Pitcher, M.R., Hicks, J., Suzuki, A., Iwata, J., Quevado, J., and Lou, Y. (2017). Interleukin33 deficiency causes tau abnormality and neurodegeneration with Alzheimer-like symptoms in aged mice. Transl. Psychiatry *7*, e1164–e1164.

Carretero, J., Sánchez-Robledo, V., Carretero-Hernández, M., Catalano-Iniesta, L., García-Barrado, M.J., Iglesias-Osma, M.C., and Blanco, E.J. (2019). Prolactin system in the hippocampus. Cell Tissue Res. *375*, 193–199.

Carson, M.J., Doose, J.M., Melchior, B., Schmid, C.D., and Ploix, C.C. (2006). CNS immune privilege: hiding in plain sight. Immunol. Rev. *213*, 48–65.

Castillo, E., Leon, J., Mazzei, G., Abolhassani, N., Haruyama, N., Saito, T., Saido, T., Hokama, M., Iwaki, T., Ohara, T., et al. (2017). Comparative profiling of cortical gene expression in Alzheimer's disease patients and mouse models demonstrates a link between amyloidosis and neuroinflammation. Sci. Rep. *7*, 17762.

De Cecco, M., Criscione, S.W., Peterson, A.L., Neretti, N., Sedivy, J.M., and Kreiling, J.A. (2013). Transposable elements become active and mobile in the genomes of aging mammalian somatic tissues. Aging (Albany. NY). *5*, 867–883.

De Cecco, M., Ito, T., Petrashen, A.P., Elias, A.E., Skvir, N.J., Criscione, S.W., Caligiana, A., Brocculi, G., Adney, E.M., Boeke, J.D., et al. (2019). L1 drives IFN in senescent cells and promotes age-associated inflammation. Nature *566*, 73–78.

Chen, W. V, and Maniatis, T. (2013). Clustered protocadherins. Development *140*, 3297–3302.

Chen, X., Yang, H., Zhou, X., Zhang, L., and Lu, X. (2016). MiR-93 Targeting EphA4 Promotes

Neurite Outgrowth from Spinal Cord Neurons. J. Mol. Neurosci. *58*, 517–524.

Choi, J.H., and Won, M.-H. (2011). Microglia in the normally aged hippocampus. Lab. Anim. Res. *27*, 181–187.

Consortium, T.E.P. (2012). An integrated encyclopedia of DNA elements in the human genome. Nature *489*, 57–74.

Cordaux, R., and Batzer, M.A. (2009). The impact of retrotransposons on human genome evolution. Nat. Rev. Genet. *10*, 691–703.

Darbelli, L., Choquet, K., Richard, S., and Kleinman, C.L. (2017). Transcriptome profiling of mouse brains with qkI-deficient oligodendrocytes reveals major alternative splicing defects including self-splicing. Sci. Rep. *7*, 7554.

Dityatev, A., and Schachner, M. (2003). Extracellular matrix molecules and synaptic plasticity. Nat. Rev. Neurosci. *4*, 456–468.

Dobin, A., Davis, C.A., Schlesinger, F., Drenkow, J., Zaleski, C., Jha, S., Batut, P., Chaisson, M., and Gingeras, T.R. (2013). STAR: ultrafast universal RNA-seq aligner. Bioinformatics *29*, 15–21.

Eldh, M., Lötvall, J., Malmhäll, C., and Ekström, K. (2012). Importance of RNA isolation methods for analysis of exosomal RNA: evaluation of different methods. Mol. Immunol. *50*, 278–286.

Elliott, R., Li, F., Dragomir, I., Chua, M.M.W., Gregory, B.D., and Weiss, S.R. (2013). Analysis of the Host Transcriptome from Demyelinating Spinal Cord of Murine Coronavirus-Infected Mice. PLoS One *8*, e75346.

Encinas, J.M., Michurina, T. V, Peunova, N., Park, J.-H., Tordo, J., Peterson, D.A., Fishell, G., Koulakov, A., and Enikolopov, G. (2011). Division-coupled astrocytic differentiation and age-related depletion of neural stem cells in the adult hippocampus. Cell Stem Cell *8*, 566–579.

Fauré, J., Lachenal, G., Court, M., Hirrlinger, J., Chatellard-Causse, C., Blot, B., Grange, J., Schoehn, G., Goldberg, Y., Boyer, V., et al. (2006). Exosomes are released by cultured cortical neurones. Mol. Cell. Neurosci. *31*, 642–648.

Feschotte, C. (2008). Transposable elements and the evolution of regulatory networks. Nat. Rev. Genet. *9*, 397–405.

Fischer, A., Sananbenesi, F., Wang, X., Dobbin, M., and Tsai, L.-H. (2007). Recovery of learning and memory is associated with chromatin remodelling. Nature *447*, 178–182.

Fjell, A.M., Walhovd, K.B., Fennema-Notestine, C., McEvoy, L.K., Hagler, D.J., Holland, D., Brewer, J.B., and Dale, A.M. (2009). One-year brain atrophy evident in healthy aging. J. Neurosci. *29*, 15223–15231.

Frankland, P.W., and Bontempi, B. (2005). The organization of recent and remote memories. Nat. Rev. Neurosci. *6*, 119–130.

Frühbeis, C., Fröhlich, D., Kuo, W.P., Amphornrat, J., Thilemann, S., Saab, A.S., Kirchhoff, F., Möbius, W., Goebbels, S., Nave, K.-A., et al. (2013). Neurotransmitter-Triggered Transfer of Exosomes Mediates Oligodendrocyte–Neuron Communication. PLoS Biol. *11*, e1001604.

Fujita, N., Sato, S., Ishiguro, H., Inuzuka, T., Baba, H., Kurihara, T., Takahashi, Y., and Miyatake, T. (1990). The Large Isoform of Myelin-Associated Glycoprotein Is Scarcely Expressed in the Quaking Mouse Brain. J. Neurochem. *55*, 1056–1059.

Goelet, P., Castellucci, V.F., Schacher, S., and Kandel, E.R. (1986). The long and the short of long–term memory—a molecular framework. Nature *322*, 419–422.

Gong, X., Zhang, K., Wang, Y., Wang, J., Cui, Y., Li, S., and Luo, Y. (2013). MicroRNA-130b targets Fmr1 and regulates embryonic neural progenitor cell proliferation and differentiation. Biochem. Biophys. Res. Commun. *439*, 493–500.

Goyal, M.S., Blazey, T.M., Su, Y., Couture, L.E., Durbin, T.J., Bateman, R.J., Benzinger, T.L.-S., Morris, J.C., Raichle, M.E., and Vlassenko, A.G. (2019). Persistent metabolic youth in the aging female brain. Proc. Natl. Acad. Sci. U. S. A. *116*, 3251–3255.

Guduric-Fuchs, J., O'Connor, A., Camp, B., O'Neill, C.L., Medina, R.J., and Simpson, D.A. (2012). Selective extracellular vesicle-mediated export of an overlapping set of microRNAs from multiple cell types. BMC Genomics *13*, 357.

El Hajj, N., Dittrich, M., and Haaf, T. (2017). Epigenetic dysregulation of protocadherins in human disease. Semin. Cell Dev. Biol. *69*, 172–182.

Han, P., and Chang, C.-P. (2015). Long non-coding RNA and chromatin remodeling. RNA Biol. *12*, 1094–1098.

HÄNNINEN, T., KOIVISTO, K., REINIKAINEN, K.J., HELKALA, E.-L., SOININEN, H., MYKKÄNEN, L., LAAKSO, M., and RIEKKINEN, P.J. (1996). Prevalence of Ageing-associated Cognitive Decline in an Elderly Population. Age Ageing *25*, 201–205.

Harada, C.N., Natelson Love, M.C., and Triebel, K.L. (2013). Normal cognitive aging. Clin. Geriatr. Med. *29*, 737–752.

Harding, C., and Stahl, P. (1983). Transferrin recycling in reticulocytes: pH and iron are important determinants of ligand binding and processing. Biochem. Biophys. Res. Commun. *113*, 650–658.

Harding, C. V, Heuser, J.E., and Stahl, P.D. (2013). Exosomes: looking back three decades and into the future. J. Cell Biol. *200*, 367–371.

Hass, J., Walton, E., Kirsten, H., Turner, J., Wolthusen, R., Roessner, V., Sponheim, S.R., Holt, D., Gollub, R., Calhoun, V.D., et al. (2015). Complexin2 modulates working memory-related neural activity in patients with schizophrenia. Eur. Arch. Psychiatry Clin. Neurosci. *265*, 137–145.

Haure-Mirande, J.-V., Audrain, M., Fanutza, T., Kim, S.H., Klein, W.L., Glabe, C., Readhead, B., Dudley, J.T., Blitzer, R.D., Wang, M., et al. (2017). Deficiency of TYROBP, an adapter protein for TREM2 and CR3 receptors, is neuroprotective in a mouse model of early Alzheimer's pathology. Acta Neuropathol. *134*, 769–788.

Hayden, K.M., Reed, B.R., Manly, J.J., Tommet, D., Pietrzak, R.H., Chelune, G.J., Yang, F.M., Revell, A.J., Bennett, D.A., and Jones, R.N. (2011). Cognitive decline in the elderly: an analysis of population heterogeneity. Age Ageing *40*, 684–689.

Heinz, S., Benner, C., Spann, N., Bertolino, E., Lin, Y.C., Laslo, P., Cheng, J.X., Murre, C., Singh, H., and Glass, C.K. (2010). Simple Combinations of Lineage-Determining Transcription Factors Prime cis-Regulatory Elements Required for Macrophage and B Cell Identities. Mol. Cell *38*, 576–589.

Herbst, W.A., and Martin, K.C. (2017). Regulated transport of signaling proteins from synapse to nucleus. Curr. Opin. Neurobiol. *45*, 78–84.

Ho, V.M., Lee, J.-A., and Martin, K.C. (2011). The cell biology of synaptic plasticity. Science *334*, 623–628.

Hong, S., Beja-Glasser, V.F., Nfonoyim, B.M., Frouin, A., Li, S., Ramakrishnan, S., Merry, K.M., Shi, Q., Rosenthal, A., Barres, B.A., et al. (2016). Complement and microglia mediate early synapse loss in Alzheimer mouse models. Science *352*, 712–716.

Hood, J.L., San, R.S., and Wickline, S.A. (2011). Exosomes Released by Melanoma Cells Prepare Sentinel Lymph Nodes for Tumor Metastasis. Cancer Res. *71*, 3792–3801.

Hooper, J.E. (2014). A survey of software for genome-wide discovery of differential splicing in RNA-Seq data. Hum. Genomics *8*, 3.

Hu, Z., and Li, Z. (2017). miRNAs in synapse development and synaptic plasticity. Curr. Opin. Neurobiol. *45*, 24–31.

Huang, D.W., Sherman, B.T., and Lempicki, R.A. (2009a). Bioinformatics enrichment tools: paths toward the comprehensive functional analysis of large gene lists. Nucleic Acids Res. *37*, 1–13.

Huang, D.W., Sherman, B.T., and Lempicki, R.A. (2009b). Systematic and integrative analysis of large gene lists using DAVID bioinformatics resources. Nat. Protoc. *4*, 44–57.

Ishimoto, T., Ninomiya, K., Inoue, R., Koike, M., Uchiyama, Y., and Mori, H. (2017). Mice lacking BCAS1, a novel myelin-associated protein, display hypomyelination, schizophrenia-like abnormal behaviors, and upregulation of inflammatory genes in the brain. Glia *65*, 727–739.

Ishizu, H., Siomi, H., and Siomi, M.C. (2012). Biology of PIWI-interacting RNAs: new insights into biogenesis and function inside and outside of germlines. Genes Dev. *26*, 2361–2373.

Jauhari, A., Singh, T., and Yadav, S. (2018). Expression of miR-145 and Its Target Proteins Are Regulated by miR-29b in Differentiated Neurons. Mol. Neurobiol. *55*, 8978–8990.

Johnson, W.E., Li, C., and Rabinovic, A. (2007). Adjusting batch effects in microarray expression data using empirical Bayes methods. Biostatistics *8*, 118–127.

Johnstone, R.M. (2006). Exosomes biological significance: A concise review. Blood Cells, Mol. Dis. *36*, 315–321.

Klemm, S.L., Shipony, Z., and Greenleaf, W.J. (2019). Chromatin accessibility and the regulatory epigenome. Nat. Rev. Genet. *20*, 207–220.

Kohman, R.A., Rodriguez-Zas, S.L., Southey, B.R., Kelley, K.W., Dantzer, R., and Rhodes, J.S. (2011). Voluntary Wheel Running Reverses Age-Induced Changes in Hippocampal Gene Expression. PLoS One *6*, e22654.

Koles, K., Nunnari, J., Korkut, C., Barria, R., Brewer, C., Li, Y., Leszyk, J., Zhang, B., and Budnik, V. (2012). Mechanism of evenness interrupted (Evi)-exosome release at synaptic boutons. J. Biol. Chem. *287*, 16820–16834.

Korkut, C., Li, Y., Koles, K., Brewer, C., Ashley, J., Yoshihara, M., and Budnik, V. (2013). Regulation of postsynaptic retrograde signaling by presynaptic exosome release. Neuron *77*, 1039–1046.

De La Torre-Ubieta, L., Stein, J.L., Won, H., Opland, C.K., Liang, D., Lu, D., and Geschwind Correspondence, D.H. (2018). The Dynamic Landscape of Open Chromatin during Human Cortical Neurogenesis.

Lachenal, G., Pernet-Gallay, K., Chivet, M., Hemming, F.J., Belly, A., Bodon, G., Blot, B., Haase, G., Goldberg, Y., and Sadoul, R. (2011). Release of exosomes from differentiated neurons and its regulation by synaptic glutamatergic activity. Mol. Cell. Neurosci. *46*, 409–418.

Lane, R.E., Korbie, D., Hill, M.M., and Trau, M. (2018). Extracellular vesicles as circulating cancer biomarkers: opportunities and challenges. Clin. Transl. Med. *7*, 14.

León, I., Tascón, L., and Cimadevilla, J.M. (2016). Age and gender-related differences in a spatial memory task in humans. Behav. Brain Res. *306*, 8–12.

Li, H., and Durbin, R. (2009). Fast and accurate short read alignment with Burrows-Wheeler transform. Bioinformatics *25*, 1754–1760.

Li, B., Carey, M., and Workman, J.L. (2007). The role of chromatin during transcription. Cell *128*, 707–719.

Li, P., Kaslan, M., Lee, S.H., Yao, J., and Gao, Z. (2017). Progress in Exosome Isolation Techniques. Theranostics *7*, 789–804.

Liao, Y., Smyth, G.K., and Shi, W. (2014). featureCounts: an efficient general purpose program for assigning sequence reads to genomic features. Bioinformatics *30*, 923–930.

Liu, H.-Y., Huang, C.-M., Hung, Y.-F., and Hsueh, Y.-P. (2015). The microRNAs Let7c and miR21 are recognized by neuronal Toll-like receptor 7 to restrict dendritic growth of neurons. Exp. Neurol. *269*, 202–212.

Liu, K., Lei, R., Li, Q., Wang, X.-X., Wu, Q., An, P., Zhang, J., Zhu, M., Xu, Z., Hong, Y., et al. (2016). Transferrin Receptor Controls AMPA Receptor Trafficking Efficiency and Synaptic Plasticity. Sci. Rep. *6*, 21019.

Lloyd, A.F., and Miron, V.E. (2019). The pro-remyelination properties of microglia in the central nervous system. Nat. Rev. Neurol. *15*, 447–458.

Love, M.I., Huber, W., and Anders, S. (2014). Moderated estimation of fold change and dispersion for RNA-seq data with DESeq2. Genome Biol. *15*, 550.

Lucin, K.M., and Wyss-Coray, T. (2009). Immune activation in brain aging and neurodegeneration: too much or too little? Neuron *64*, 110–122.

Mazin, P., Xiong, J., Liu, X., Yan, Z., Zhang, X., Li, M., He, L., Somel, M., Yuan, Y., Phoebe Chen, Y., et al. (2013). Widespread splicing changes in human brain development and aging. Mol. Syst. Biol. *9*, 633.

McCarrey, A.C., An, Y., Kitner-Triolo, M.H., Ferrucci, L., and Resnick, S.M. (2016). Sex differences in cognitive trajectories in clinically normal older adults. Psychol. Aging *31*, 166–175.

McKenzie, A.T., Wang, M., Hauberg, M.E., Fullard, J.F., Kozlenkov, A., Keenan, A., Hurd, Y.L., Dracheva, S., Casaccia, P., Roussos, P., et al. (2018). Brain Cell Type Specific Gene Expression and Co-expression Network Architectures. Sci. Rep. *8*, 8868.

Van Meter, M., Kashyap, M., Rezazadeh, S., Geneva, A.J., Morello, T.D., Seluanov, A., and Gorbunova, V. (2014). SIRT6 represses LINE1 retrotransposons by ribosylating KAP1 but this repression fails with stress and age. Nat. Commun. *5*, 5011.

Mora, A., Sandve, G.K., Gabrielsen, O.S., and Eskeland, R. (2016). In the loop: promoter-enhancer interactions and bioinformatics. Brief. Bioinform. *17*, 980–995.

Morel, L., Regan, M., Higashimori, H., Ng, S.K., Esau, C., Vidensky, S., Rothstein, J., and Yang, Y. (2013). Neuronal exosomal miRNA-dependent translational regulation of astroglial glutamate transporter GLT1. J. Biol. Chem. *288*, 7105–7116.

Morelli, A.E., Larregina, A.T., Shufesky, W.J., Sullivan, M.L.G., Stolz, D.B., Papworth, G.D.,

Zahorchak, A.F., Logar, A.J., Wang, Z., Watkins, S.C., et al. (2004). Endocytosis, intracellular sorting, and processing of exosomes by dendritic cells. Blood *104*, 3257–3266.

Mulcahy, L.A., Pink, R.C., and Carter, D.R.F. (2014). Routes and mechanisms of extracellular vesicle uptake. J. Extracell. Vesicles *3*.

Muntasell, A., Berger, A.C., and Roche, P.A. (2007). T cell-induced secretion of MHC class II-peptide complexes on B cell exosomes. EMBO J. *26*, 4263–4272.

Nave, K.-A., and Werner, H.B. (2014). Myelination of the Nervous System: Mechanisms and Functions. Annu. Rev. Cell Dev. Biol. *30*, 503–533.

Nicholson, D.A., Yoshida, R., Berry, R.W., Gallagher, M., and Geinisman, Y. (2004). Reduction in size of perforated postsynaptic densities in hippocampal axospinous synapses and age-related spatial learning impairments. J. Neurosci. *24*, 7648–7653.

van Niel, G., Porto-Carreiro, I., Simoes, S., and Raposo, G. (2006). Exosomes: a common pathway for a specialized function. J. Biochem. *140*, 13–21.

Nuriya, M., and Huganir, R.L. (2006). Regulation of AMPA receptor trafficking by N-cadherin. J. Neurochem. *97*, 652–661.

Pal, S., and Tyler, J.K. (2016). Epigenetics and aging. Sci. Adv. *2*, e1600584.

Palmer, A.L., and Ousman, S.S. (2018). Astrocytes and Aging. Front. Aging Neurosci. *10*, 337.

Pan, B.-T., and Johnstone, R.M. (1983). Fate of the transferrin receptor during maturation of sheep reticulocytes in vitro: Selective externalization of the receptor. Cell *33*, 967–978.

Pastuzyn, E.D., Day, C.E., Kearns, R.B., Kyrke-Smith, M., Taibi, A. V., McCormick, J., Yoder, N., Belnap, D.M., Erlendsson, S., Morado, D.R., et al. (2018). The Neuronal Gene Arc Encodes a Repurposed Retrotransposon Gag Protein that Mediates Intercellular RNA Transfer. Cell *172*, 275-288.e18.

Pawlowski, T.L., Bellush, L.L., Wright, A.W., Walker, J.P., Colvin, R.A., and Huentelman, M.J. (2009). Hippocampal gene expression changes during age-related cognitive decline. Brain Res. *1256*, 101–110.

Pegtel, D.M., Cosmopoulos, K., Thorley-Lawson, D.A., van Eijndhoven, M.A.J., Hopmans, E.S., Lindenberg, J.L., de Gruijl, T.D., Würdinger, T., and Middeldorp, J.M. (2010). Functional delivery of viral miRNAs via exosomes. Proc. Natl. Acad. Sci. U. S. A. *107*, 6328–6333.

Penner, M.R., Roth, T.L., Chawla, M.K., Hoang, L.T., Roth, E.D., Lubin, F.D., Sweatt, J.D., Worley, P.F., and Barnes, C.A. (2011). Age-related changes in Arc transcription and DNA methylation within the hippocampus. Neurobiol. Aging *32*, 2198–2210.

Peters, A. (2002). The effects of normal aging on myelin and nerve fibers: A review. J. Neurocytol. *31*, 581–593.

Petralia, R.S., Mattson, M.P., and Yao, P.J. (2014). Communication breakdown: the impact of ageing on synapse structure. Ageing Res. Rev. *14*, 31–42.

Pruessner, J.C., Collins, D.L., Pruessner, M., and Evans, A.C. (2001). Age and gender predict volume decline in the anterior and posterior hippocampus in early adulthood. J. Neurosci. *21*, 194–200.

Qiu, J., Dunbar, D.R., Noble, J., Cairns, C., Carter, R., Kelly, V., Chapman, K.E., Seckl, J.R., and Yau, J.L.W. (2016). Decreased Npas4 and Arc mRNA Levels in the Hippocampus of Aged Memory-Impaired Wild-Type But Not Memory Preserved 11β-HSD1 Deficient Mice. J. Neuroendocrinol. *28*, n/a.

Raj, T., Li, Y.I., Wong, G., Humphrey, J., Wang, M., Ramdhani, S., Wang, Y.-C., Ng, B., Gupta, I., Haroutunian, V., et al. (2018). Integrative transcriptome analyses of the aging brain implicate altered splicing in Alzheimer's disease susceptibility. Nat. Genet. *50*, 1584–1592.

Rajasethupathy, P., Antonov, I., Sheridan, R., Frey, S., Sander, C., Tuschl, T., and Kandel, E.R. (2012). A Role for Neuronal piRNAs in the Epigenetic Control of Memory-Related Synaptic Plasticity. Cell *149*, 693–707.

Rajendran, L., Bali, J., Barr, M.M., Court, F.A., Krämer-Albers, E.-M., Picou, F., Raposo, G., van der Vos, K.E., van Niel, G., Wang, J., et al. (2014). Emerging roles of extracellular vesicles in the nervous system. J. Neurosci. *34*, 15482–15489.

Rangwala, S.H., Zhang, L., and Kazazian, H.H. (2009). Many LINE1 elements contribute to the transcriptome of human somatic cells. Genome Biol. *10*, R100.

Raposo, G., and Stoorvogel, W. (2013a). Extracellular vesicles: exosomes, microvesicles, and friends. J. Cell Biol. *200*, 373–383.

Raposo, G., and Stoorvogel, W. (2013b). Extracellular vesicles: exosomes, microvesicles, and friends. J. Cell Biol. *200*, 373–383.

Richardson, S.R., Doucet, A.J., Kopera, H.C., Moldovan, J.B., Garcia-Perez, J.L., and Moran, J. V (2015). The Influence of LINE-1 and SINE Retrotransposons on Mammalian Genomes. Microbiol. Spectr. *3*, MDNA3-0061–2014.

Robinson, M.D., and Oshlack, A. (2010). A scaling normalization method for differential expression analysis of RNA-seq data. Genome Biol. *11*, R25.

Robinson, M.D., McCarthy, D.J., and Smyth, G.K. (2010). edgeR: a Bioconductor package for differential expression analysis of digital gene expression data. Bioinformatics *26*, 139–140.

Rowe, W.B., Blalock, E.M., Chen, K.-C., Kadish, I., Wang, D., Barrett, J.E., Thibault, O., Porter, N.M., Rose, G.M., and Landfield, P.W. (2007). Hippocampal expression analyses reveal selective association of immediate-early, neuroenergetic, and myelinogenic pathways with cognitive impairment in aged rats. J. Neurosci. *27*, 3098–3110.

Santos, G., Barateiro, A., Gomes, C.M., Brites, D., and Fernandes, A. (2018). Impaired oligodendrogenesis and myelination by elevated S100B levels during neurodevelopment. Neuropharmacology *129*, 69–83.

Satoh, J., Kino, Y., Asahina, N., Takitani, M., Miyoshi, J., Ishida, T., and Saito, Y. (2016). TMEM119 marks a subset of microglia in the human brain. Neuropathology *36*, 39–49.

Schneider, A., and Simons, M. (2013). Exosomes: vesicular carriers for intercellular communication in neurodegenerative disorders. Cell Tissue Res. *352*, 33–47.

Shaftel, S.S., Griffin, W.S.T., and O'Banion, M.K. (2008). The role of interleukin-1 in neuroinflammation and Alzheimer disease: an evolving perspective. J. Neuroinflammation *5*, 7.

Shankar, S., Teyler, T.J., and Robbins, N. (1998). Aging Differentially Alters Forms of Long-Term Potentiation in Rat Hippocampal Area CA1. J. Neurophysiol. *79*, 334–341.

Sharma, P., Mesci, P., Carromeu, C., McClatchy, D.R., Schiapparelli, L., Yates, J.R., Muotri, A.R., and Cline, H.T. (2019). Exosomes regulate neurogenesis and circuit assembly. Proc. Natl. Acad. Sci. U. S. A. *116*, 16086–16094.

Shen, S., Park, J.W., Lu, Z., Lin, L., Henry, M.D., Wu, Y.N., Zhou, Q., and Xing, Y. (2014). rMATS: robust and flexible detection of differential alternative splicing from replicate RNA-Seq data. Proc. Natl. Acad. Sci. U. S. A. *111*, E5593-601.

Slieker, R.C., van Iterson, M., Luijk, R., Beekman, M., Zhernakova, D. V., Moed, M.H., Mei, H., van Galen, M., Deelen, P., Bonder, M.J., et al. (2016). Age-related accrual of methylomic variability is linked to fundamental ageing mechanisms. Genome Biol. *17*, 191.

Soreq, L., UK Brain Expression Consortium, U.B.E., North American Brain Expression Consortium, N.A.B.E., Rose, J., Soreq, E., Hardy, J., Trabzuni, D., Cookson, M.R., Smith, C., Ryten, M., et al. (2017). Major Shifts in Glial Regional Identity Are a Transcriptional Hallmark of Human Brain Aging. Cell Rep. *18*, 557–570.

Sorrells, S.F., Paredes, M.F., Cebrian-Silla, A., Sandoval, K., Qi, D., Kelley, K.W., James, D., Mayer, S., Chang, J., Auguste, K.I., et al. (2018). Human hippocampal neurogenesis drops sharply in children to undetectable levels in adults. Nature *555*, 377–381.

Stilling, R.M., Benito, E., Barth, J., Gertig, M., Capece, V., Burckhardt, S., Bonn, S., and Fischer, A. (2014). De-regulation of gene expression and alternative splicing affects distinct cellular pathways in the aging hippocampus. Front. Cell. Neurosci. *8*, 373.

Su, Y., Shin, J., Zhong, C., Wang, S., Roychowdhury, P., Lim, J., Kim, D., Ming, G.-L., and Song, H. (2017). Neuronal activity modifies the chromatin accessibility landscape in the adult brain. Nat. Neurosci. *20*, 476–483.

Tai, C.-Y., Kim, S.A., and Schuman, E.M. (2008). Cadherins and synaptic plasticity. Curr. Opin. Cell Biol. *20*, 567–575.

Taylor, D.D., and Gercel-Taylor, C. (2008). MicroRNA signatures of tumor-derived exosomes as diagnostic biomarkers of ovarian cancer. Gynecol. Oncol. *110*, 13–21.

Théry, C., Zitvogel, L., and Amigorena, S. (2002). Exosomes: composition, biogenesis and function. Nat. Rev. Immunol. *2*, 569–579.

Torner, L. (2016). Actions of Prolactin in the Brain: From Physiological Adaptations to Stress and Neurogenesis to Psychopathology. Front. Endocrinol. (Lausanne). *7*, 25.

Trabzuni, D., Ramasamy, A., Imran, S., Walker, R., Smith, C., Weale, M.E., Hardy, J., Ryten, M., and Consortium, N.A.B.E. (2013). Widespread sex differences in gene expression and splicing in the adult human brain. Nat. Commun. *4*, 2771.

Tropak, M.B., Johnson, P.W., Dunn, R.J., and Roder, J.C. (1988). Differential splicing of MAG transcripts during CNS and PNS development. Mol. Brain Res. *4*, 143–155.

Tsurumi, A., and Li, W. (2012). Global heterochromatin loss. Epigenetics *7*, 680–688.

Uddin, R.K., and Singh, S.M. (2013). Hippocampal gene expression meta-analysis identifies aging and age-associated spatial learning impairment (ASLI) genes and pathways. PLoS One *8*, e69768.

Valadi, H., Ekstrom, K., Bossios, A., Sjostrand, M., Lee, J.J., and Lotvall, J.O. (2007). Exosome-mediated transfer of mRNAs and microRNAs is a novel mechanism of genetic exchange between cells. Nat Cell Biol *9*, 654–659.

Villarroya-Beltri, C., Gutiérrez-Vázquez, C., Sánchez-Cabo, F., Pérez-Hernández, D., Vázquez, J., Martin-Cofreces, N., Martinez-Herrera, D.J., Pascual-Montano, A., Mittelbrunn, M., and Sánchez-Madrid, F. (2013). Sumoylated hnRNPA2B1 controls the sorting of miRNAs into exosomes through binding to specific motifs. Nat. Commun. *4*, 2980.

Villeponteau, B. (1997). The heterochromatin loss model of aging. Exp. Gerontol. *32*, 383–394.

Viña, J., and Lloret, A. (2010). Why Women Have More Alzheimer's Disease Than Men: Gender and Mitochondrial Toxicity of Amyloid-β Peptide. J. Alzheimer's Dis. *20*, S527–S533.

Wang, L., Tian, T., and Alzheimer's Disease Neuroimaging Initiative, A.D.N. (2018). Gender Differences in Elderly With Subjective Cognitive Decline. Front. Aging Neurosci. *10*, 166.

Weick, E.-M., and Miska, E.A. (2014). piRNAs: from biogenesis to function. Development *141*, 3458–3471.

White, R.E., and Giffard, R.G. (2012). MicroRNA-320 induces neurite outgrowth by targeting ARPP-19. Neuroreport *23*, 590–595.

WOODRUFF, R.H., and FRANKLIN, R.J.M. (1998). The expression of myelin basic protein exon 1 and exon 2 containing transcripts during myelination of the neonatal rat spinal cord<197>an in situ hybridization study. J. Neurocytol. *27*, 683–693.

Wu, J.I., Reed, R.B., Grabowski, P.J., and Artzt, K. (2002). Function of quaking in myelination: regulation of alternative splicing. Proc. Natl. Acad. Sci. U. S. A. *99*, 4233–4238.

Wubbolts, R., Leckie, R.S., Veenhuizen, P.T.M., Schwarzmann, G., Möbius, W., Hoernschemeyer, J., Slot, J.-W., Geuze, H.J., and Stoorvogel, W. (2003). Proteomic and biochemical analyses of human B cell-derived exosomes. Potential implications for their function and multivesicular body formation. J. Biol. Chem. *278*, 10963–10972.

XIE, F., LIANG, P., FU, H., ZHANG, J.-C., and CHEN, J. (2014). Effects of normal aging on myelin sheath ultrastructures in the somatic sensorimotor system of rats. Mol. Med. Rep. *10*, 459–466.

Xu, J., Kobayashi, S., Yamaguchi, S., Iijima, K., Okada, K., and Yamashita, K. (2000). Gender Effects on Age-Related Changes in Brain Structure. Am. J. Neuroradiol. *21*.

Yagi, T. (2012). Molecular codes for neuronal individuality and cell assembly in the brain. Front. Mol. Neurosci. *5*, 45.

Yang, S., Li, C., Zhang, W., Wang, W., and Tang, Y. (2008). Sex differences in the white matter and myelinated nerve fibers of Long-Evans rats. Brain Res. *1216*, 16–23.

Yuan, T., Huang, X., Woodcock, M., Du, M., Dittmar, R., Wang, Y., Tsai, S., Kohli, M., Boardman, L., Patel, T., et al. (2016). Plasma extracellular RNA profiles in healthy and cancer patients. Sci. Rep. *6*, 19413.

Zhang, J., Li, S., Li, L., Li, M., Guo, C., Yao, J., and Mi, S. (2015). Exosome and Exosomal MicroRNA: Trafficking, Sorting, and Function. Genomics. Proteomics Bioinformatics *13*, 17–24.

Zhang, Y., Liu, T., Meyer, C.A., Eeckhoute, J., Johnson, D.S., Bernstein, B.E., Nussbaum, C., Myers, R.M., Brown, M., Li, W., et al. (2008). Model-based Analysis of ChIP-Seq (MACS). Genome Biol. *9*, R137.

Zhang, Y., Chen, M., Qiu, Z., Hu, K., McGee, W., Chen, X., Liu, J., Zhu, L., and Wu, J.Y. (2016). MiR-130a regulates neurite outgrowth and dendritic spine density by targeting MeCP2. Protein Cell *7*, 489–500.

Zitvogel, L., Regnault, A., Lozier, A., Wolfers, J., Flament, C., Tenza, D., Ricciardi-Castagnoli, P.,

Raposo, G., and Amigorena, S. (1998). Eradication of established murine tumors using a novel cell-free vaccine: dendritic cell derived exosomes. Nat. Med. *4*, 594–600.

Zöller, M. (2009). Tetraspanins: push and pull in suppressing and promoting metastasis. Nat. Rev. Cancer *9*, 40–55.